FATIGUE EQUIVALENT STATIC LOAD: METHODOLOGY FOR THE DESIGN OF VEHICLE STRUCTURES

Etienne Pieter Willem Prinsloo

Submitted in partial fulfilment of the
requirements for the degree

Master of Engineering

in the

Faculty of Engineering, Built Environment
and Information Technologies,
University of Pretoria

February 2003

Abstract

FATIGUE EQUIVALENT STATIC LOAD: METHODOLOGY FOR THE DESIGN OF VEHICLE STRUCTURES

by

Etienne Pieter Willem Prinsloo

Advisor: J. Wannenburg

Department of Mechanical and Aeronautical Engineering

Master of Engineering

Keywords: vehicle structures, fatigue loads, FESL, structural design, damage, finite element analysis, durability, cost effective, measurements

This study is concerned with the design of vehicle structures through the use of Fatigue Equivalent Static Loads (FESL). A large percentage of failures of mechanical structures can be attributed to fatigue. Furthermore, it is also generally accepted that defective structural design is mostly caused by insufficient knowledge of the input loading. The fatigue loads experienced by vehicle structures are especially difficult to quantify. In the current competitive markets, it is essential to use a pro-active, timely and cost effective process to solve fatigue related problems. The heart of the FESL methodology is the ability to condense a large amount of input load data into a single fatigue load. This is achieved by calculating the damage of the measurements and converting it to an equivalent stress, through the use of a calibration matrix obtained from a unit-load finite element analysis. A Fatigue Equivalent Static Load can now be determined, and the vehicle structure can be evaluated for durability.

Samevatting

VERMOEIDHEID EKWIVALENTE STATIESE BELASTING: METODIEK VIR DIE ONTWERP VAN VOERTUIG STRUKTURE

deur

Etienne Pieter Willem Prinsloo

Studieleier: J. Wannenburg

Departement van Meganiese en Lugvaartkundige Ingenieurswese

Magister in Ingenieurswese

Sleutelterme: voertuig strukture, belastings, VESB, strukture ontwerp, vermoeidheidskade, eindige element analise, koste effektiwiteit, metings

Die studie handel oor die ontwerp van voertuig strukture deur gebruik te maak van die Vermoeidheid Ekwivalente Statiese Belasting (VESB) metodiek. 'n Groot persentasie van falings in meganiese strukture kan toegeskryf word aan vermoeidheid. Verder, word dit ook algemeen aanvaar dat oneffektiewe struktuur ontwerpe hoofsaaklik te danke is aan onvoldoende kennis van die inset belastings. Die inset belastings wat voertuie ervaar is veral moeilik om te kwantifiseer. In die hedendaagse kompeterende markte is dit belangrik om 'n pro-aktiewe, tydige and koste-effektiewe proses te gebruik om vermoeidheidsprobleme op te los. Die kern van die VESB metode is die proses om groot hoeveelhede belastingsdata te kondenseer na 'n enkele vermoeidheidsbelasting. Die VESB word afgelei deur die berekende skade van die metings te gebruik

om die ekwivalente spanning af te lei. Deur gebruik te maak van 'n kalibrasie matriks, verkry deur middel van 'n eenheidsbelaste eindige element analise, kan die ekwivalente spanning en gevolglik die VESB belasting bereken word. Die meganiese struktuur kan nou geëvalueer word vir vermoeidheidskade.

Acknowledgments

I would like to thank the following people for their contributions to this study:

- My advisor and friend, Johann Wannenburg. His guidance and fruitful discussions made this study a rewarding experience.
- The *BKS Advantech Company*, for allowing and encouraging me, to proceed with my studies. The usage of their equipment proved invaluable for the case-studies in this thesis.
- The personnel at the companies, *Ford South Africa*, *DaimlerChrysler SA*, *Duncanmec* and *debis Fleet management*, for their support during the various case-studies.
- Roelof Minnaar, De Wet Strydom, Cobus Roussouw, Neels van der Merwe and the other personnel at BKS Advantech for their support and advice during the study.
- Oom Stef Ferreria, for his assistance in reviewing the thesis.
- Aldi, my wife, for her support and sacrifices throughout the study.
- And finally, my parents, their guidance and love made this thesis possible.

Contents

List of Figures

List of Tables

List of symbols

$[M]$	mass matrix
$\{\ddot{D}\}$	node acceleration vector
$\{\dot{D}\}$	node velocity vector
$\{d\}$	node displacement vector
$\{f\}$	applied nodal load vector
$\{f_t\}$	Applied time-varying nodal load vector
$[C]$	damping matrix
$[K]$	stiffness matrix
a	crack length
a_{cal}	calibration or acceleration load
a_{eqv}	equivalent acceleration load
b	Basquin's fatigue strength exponent
C	constant relating to the SN-curve (fatigue ductility coefficient)
c	fatigue ductility exponent
D_{tot}	total damage
D_i	damage fraction
E	Young's elasticity modulus
$f(g)$	correction factor that depends on geometry, loading and crack shape
ΔF_{eqv}	fatigue equivalent static load
F_{FEA}	applied FEA force
F_{meas}	measured forces
F_{unit}	unit load
ΔK	stress intensity range
K_ϵ	local strain concentration factor
K_σ	local stress concentration factor
K_t	theoretical stress concentration factor
L_c	calculated fatigue life
n_{eqv}	equivalent number of cycles

$2N_f$	number of reversals to failure
N_i	number cycles to failure
n_i	number of load cycles
s_{fail}	distance to failure
S_{cal}	calibration FEA stress
S_{FEA}	calculated FEA stress
S_e	fatigue limit stress
S_u	ultimate stress
S_y	yield stress
α	angle of reference
$\Delta\epsilon_p/2$	plastic strain amplitude
ϵ	strain
ϵ'_f	fatigue ductility coefficient
$\epsilon_{a/b/c}$	measured strains
ν	Poisson ratio
$\Delta\sigma$	stress range
$\Delta\sigma_{eqv}$	equivalent stress range
σ'_f	fatigue strength coefficient
$\sigma_{1/2}$	principal stresses
σ_{eqv}	equivalent stress
σ_a	stress amplitude
σ_f	fracture stress
σ_m	mean stress
σ_n	remote nominal stress applied to the component
τ_{max}	maximum shear stress

List of acronyms

AFNOR	Association Fracaise de Normalisation
ARMA	Autoregressive Moving Average
ASTM	American Society of Testing and Materials
BS	British Standard
CAD	Computer Aided Design
ECCS	European Convention for Constructional Steelwork
FDRS	Fatigue Damage Response Spectrum
FE	Finite Element
FEA	Finite Element Analysis
FEM	Finite Element Model
FESL	Fatigue Equivalent Static Design
FFT	Fast Fourier Transform
GUT	Grand Unified Theory
LEFM	Linear Elastic Fracture Mechanics
LVDT	Linear Variable Differential Transformer
MBS	Multi-Body System
MPC	Multiple Point Constraint
PSD	Power Spectral Density
RPA	Remote Parameter Analysis
SABS	South African Bureau for Standards
SAE	Society of Automotive Engineers
SN	Stress Life
SRS	Shock Response Spectrum
UKOSRP	United Kingdom Offshore Steels Research Project
VESB	Vermoeidheids Ekwivalent Statiese Belasting

Chapter 1

INTRODUCTION

> Fracture of components due to fatigue is the most common cause of service failure, ... *E. J. Hearn [19]*

The fatigue of metals has been studied for more than 150 years. During these years extensive research has been performed to quantify fatigue failures. By the 1970's fatigue analysis had become an established engineering tool. Despite all this knowledge, unintended fatigue failures continue to occur.

The design of components that are primarily subjected to constant amplitude cyclic loading, for instance a rotating shaft, is fairly trivial. However, when a structure is subjected to variable or ill-defined loads, the design of the structure could be quite difficult. Obtaining realistic and correct fatigue loads is of primary importance to perform a fatigue analysis on a structure. Wannenburg [39] argues that insufficient knowledge of input loads is the major cause of defective structural designs. Similar comments are also made by Olofsson [27], Rahman [29] and Broek [5].

The design of fatigue loaded structures is usually performed using either design codes or exhaustive durability evaluations. Many vehicle components, or structures, are usually designed through the use of prototypes that are evaluated using laboratory simulations and proving ground durability assessments. Experimental data is subsequently collected and an occurrence histogram is formed from the resulting time histories. The histogram is then scrutinized

to establish the worst fatigue loads. The structure (vehicle chassis, suspension arm, etc.) is then analysed using these loads. Another method currently being used to design structures is by the use of design codes. Design codes, for example the SABS road tanker code [36], usually make use of static loads. The loads prescribed by the codes are usually quite high (loads that will not realistically occur in the vehicle during normal usage). The codes also specify an additional factor of safety for the materials used (20% of the ultimate strength). Therefore, the design codes clearly incorporate allowance for fatigue loads.

The above-mentioned practices clearly have a few important drawbacks:

- *Design and development time.* In the current competitive markets, time is of the essence. Manufacturers and designers are pressurized to deliver properly designed products to their customers in the shortest time possible.

- *Cost.* The cost of time-consuming durability analysis can seriously affect the competitive edge of a manufacturer. Furthermore, the cost of an iterative prototype analysis, is currently getting prohibitive. This is especially true for manufacturers that need to deliver new products more frequently. Due to excessive factors of safety, the use of codes sometimes also implies a cost penalty.

- *Unrealistic fatigue loads.* The use of design codes may provide structures that could withstand fatigue loads. This is however not always the case. Olofsson [27] reports that an inspection of Swedish tank vehicles, showed that as much as 46 percent of the aluminum tank vehicles were impaired by cracks caused by fatigue. A design code, with all the safety factors, may therefore not be enough to accommodate fatigue loading.

The objective of this study is to present a methodology that overcomes or alleviates the above-mentioned drawbacks. The Fatigue Equivalent Static Load (FESL) method that is presented is an inexpensive and time efficient process to provide a point of departure in the design of a structure for fatigue

loads. More specifically, the methodology yields accurate and realistic fatigue loads which can be used in design.

The FESL method can be summarized as follows:

- Obtaining input data to the vehicle structure.
- Calculating the fatigue damage due to the measured load cases.
- Calculating fatigue equivalent static loads, through the use of finite element models.
- Analysing the durability of the structure, making use of the fatigue equivalent static loads and finite element models.

The structure of the thesis is as follows: *Chapter 2* explains the current theory and practices of fatigue, load determination and methodologies currently being used. *Chapter 3* provides a brief formulation of the Fatigue Equivalent Static Load methodology. *Chapter 4* defines the case-studies used in the thesis. *Chapter 5* discusses the methods employed to determine the input loads to the vehicle structures. *Chapter 6* discusses the fatigue calculations performed on the measurement data. *Chapter 7* defines the finite element structural analyses that were performed. *Chapter 8* presents the assessment of each case-study, making use of the FESL method. *Chapter 9* presents the conclusion of the study.

Chapter 2

CURRENT THEORY AND PRACTICE

2.1 Scope

This chapter aims to present the current theories and practices used by engineers in solving structural fatigue problems. The chapter is sub-divided into four sections. The first three sections explain the 'building blocks' that are necessary to perform a fatigue assessment, while the fourth section presents methodologies to incorporate these 'building blocks' into an engineering solution. Most practices of solving a fatigue damage problem follow these steps:

- *Determination of input loading.* To assess any structure accurately, the loads that act in on it must be determined. This section describes various methods currently being used to determine these loads.

- *Finite element structural analysis.* A load applied to a structure can cause extensive fatigue damage to the structure in question. If, however, the same load is applied to another structure, the fatigue damage could be minimal. To determine whether or not a structure will experience fatigue damage, the structure must be analysed for strength and other structural factors. A component that has a fairly simple geometry, for

example a shaft, can structurally be analysed using hand calculations (refer to Shigley [33]). However, for a more complex structure, e.g. a vehicle chassis, the finite element method must be used. This section explains the fundamentals of this method of structural analysis. It should be noted that a fatigue damage prediction can be performed using only strain gauge measurements (without the help of a structural analysis). This type of analysis is however limited to the immediate area around the strain gauge, and therefore has limited value.

- *Fundamentals of fatigue and durability.* The determination of loads acting on a structure and the knowledge of the structural response (strength, natural frequencies, etc.) is not enough to determine whether or not a structure will experience fatigue damage. The information obtained by the two previously mentioned exercises must be processed, using fatigue theories and principles. This section explains the fundamentals of the currently accepted fatigue theories.

- *Integration of measurement and analysis.* This section provides a few examples of strategies and techniques that are currently in use to determine a fatigue damage prediction. These strategies aim to incorporate the various methods previously explained to determine a solution to a structural fatigue problem.

2.2 Determination of Input Loading

The assessment of a vehicle structure requires the determination of the loads that affect the structure during usage. This section discusses the various methods that can be employed to determine these loads.

2.2.1 Time Domain

Fatigue based calculations are almost always done in the time domain, e.g. load or stress/strain data are measured along a time line. Stress versus time,

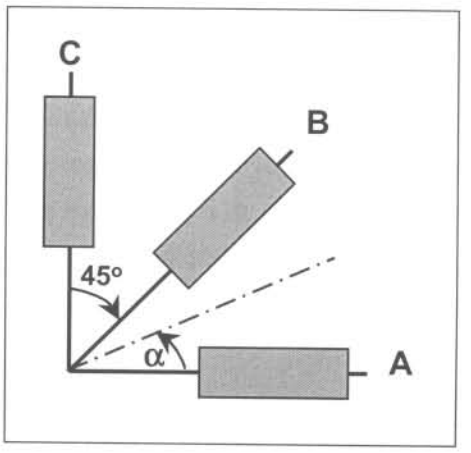

Figure 2.1: Rosette strain gauge configuration

is regarded to be in the time domain. Fatigue data and calculations are usually derived using time as the corresponding measurement unit. The Wöhler or SN curve is a plot depicting measured stress versus time. Linear Elastic Fracture Mechanics also make use of the time variable when using the Paris equation to calculate crack growth. The frequency domain is discussed later on, but all the measurements done in the case-studies make use of time domain data. Due to the importance of measuring time domain data, a few general concepts of this method will be discussed in this section.

Most of the measurements used in this study were strain gauge measurements. The purpose of strain gauge measurement is to determine the stresses and strains in any arbitrary direction on the surface of a component. This method therefore measures plane stress.

If complex loading conditions are expected, where the principle axes of the stresses are unknown, a rosette with three strain gauges is used. The rosette configuration enables the calculation of the unknown axes. Figure 2.1 shows the configuration of the three gauges that form the rosette. The principle stresses are calculated using equations 2.1 and 2.2. The direction of the principle stresses (angle α), is calculated with equation 2.3. It should be noted that if the principle loading directions are known, only two strain gauges are required. For uni-axial loading, only one strain gauge is needed. A strain

gauge can be connected to a half bridge configuration to compensate for temperature effects. When applying a strain gauge to a structure, it is vital to take the environmental influences (temperature, moisture etc.) into consideration. Neglecting these aspects, could lead to the failure of strain gauges, resulting in costly re-measurement exercises. The strain gauge measurement technique is, however, usually quite robust if correctly done.

$$\sigma_{1/2} = \frac{E}{2}\left[\frac{\epsilon_a + \epsilon_c}{1-\nu} \pm \frac{1}{1+\nu}\sqrt{2(\epsilon_a - \epsilon_b)^2 + 2(\epsilon_b - \epsilon_c)^2}\right] \quad (2.1)$$

$$\tau_{max} = \frac{E}{2(1+\nu)}\sqrt{2(\epsilon_a - \epsilon_b)^2 + 2(\epsilon_b - \epsilon_c)^2} \quad (2.2)$$

$$\tan 2\alpha = \frac{2\epsilon_b - \epsilon_a - \epsilon_c}{\epsilon_a - \epsilon_c} \quad (2.3)$$

where :

E = Young's modulus

$\sigma_{1/2}$ = Principal stresses

$\epsilon_{a/b/c}$ = Measured strains

ν = Poisson ratio

τ_{max} = Maximum shear stress

α = Angle of reference

The measurement of accelerations, forces and displacements is sometimes necessary. The integration of acceleration to velocity and subsequently, displacement, is a common procedure, but differentiation is usually avoided due to the amplification of the noise present in the data.

In the case studies presented in this thesis, the measurements of forces were sometimes done with strain gauges. The strains that were measured on the specially designated strain gauges were calibrated with a known force. If the calibration was not possible, manual calculations of the force were done

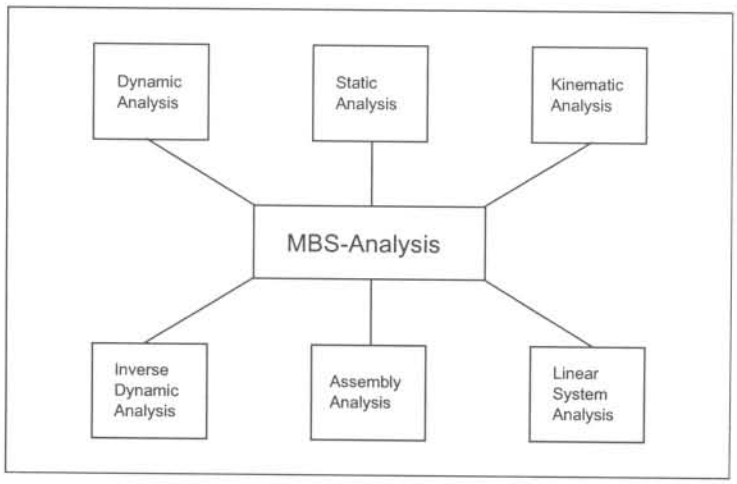

Figure 2.2: MBS: various analyses

to calculate bending or tension stresses. The strain gauges, used for force calculations, must however be positioned where the measured force will have the primary effect on the stress situation.

Forces were sometimes also measured, using a Linear Variable Differential Transformer (LVDT). The displacements of the LVDT were used in conjunction with suspension spring characteristics. The displacements can be differentiated to give velocities. The velocities can be calibrated to forces, using the characteristics of the suspensions shock absorber. More information regarding this subject can be found in [4].

2.2.2 Dynamic Simulation

Presently, the best method to obtain load information for vehicles is to use measurement recording techniques on available prototype vehicles. It would be highly desirable to be able to simulate the vehicle's behaviour over a certain terrain without an actual vehicle. Conle [11] partially solved the problem by using wheel-force recordings as inputs into a DADS vehicle dynamics simulation program. The weak links in the system are tyre models and bushing models. These areas contain components and materials that are highly non-linear. Al-

though progress has been made in these areas, at present the load-time data cannot reliably be derived from full vehicle computer simulations [10].

Gopalakrishnan [16] describes how the load-time history experienced by the vehicle, can be generated using dynamic software codes such as ADAMS. Ideally, the use of a dynamic analysis code makes the measurement process of the prototype vehicles obsolete. A vehicle or its components can thus be designed and analysed without the costly prototype methodology. Gopalakrishnan also reports that the tyre model used in ADAMS needed considerable additional work to predict the suspension loads more accurately.

Dietz [12] reports a procedure wherein a dynamic analysis is used to obtain inputs to a structure. The reported procedure makes use of a finite element method (FEM) and a multi-body system (MBS). The MBS approach makes use of various analysis features (refer to figure 2.2). The MBS method has a great advantage, in obtaining realistic load scenarios, by the use of the finite element method. The determination of time-varying boundary and load conditions can be determined by multi-body simulation. In the case of modelling a locomotive, the dynamic behaviour of the vehicle, the excitation of the track, the vehicle velocity and other operational data, influence these loads. A dynamic load ($y(t)$) can therefore be determined. These loads can be used to calculate fatigue damages of the finite element model (refer to figure 2.3). The finite element model is therefore used in the process of generating loads, as well as using these loads to evaluate the fatigue damage.

Butkunas et al [6] reports the use of a dynamic analysis to establish the inputs to a vehicle. The authors use the measured data of terrain (bump sizes, spacing, etc.) to construct an environment for the use on a dynamic, single degree of freedom system.

2.2.3 Load Spectra

The main influencing parameters on the loading of a vehicle may be defined as usage, structural behaviour (vehicle dynamic properties and design) and operational conditions. Grubisic [17] introduces a technique to determine a

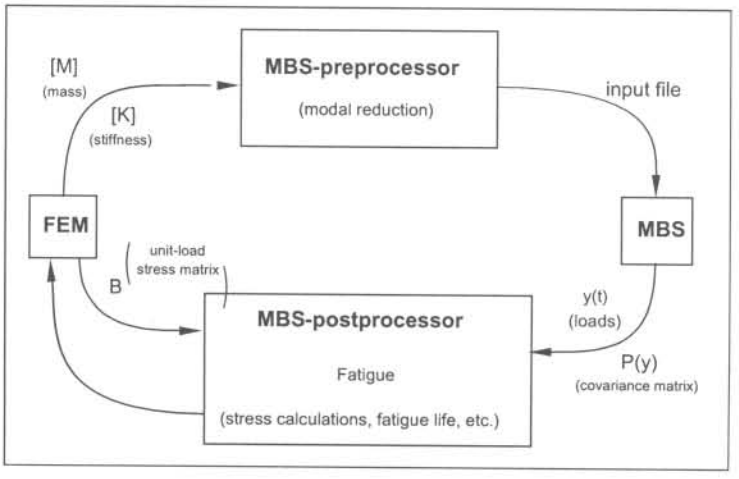

Figure 2.3: FEM-MBS interface

load spectrum of a vehicle for design and testing. The load spectra must fulfil the task of predicting the service life of a vehicle. The main parameters that influence the load spectra are depicted in figure 2.4. Figure 2.5 shows a possible design spectrum. In the figure the characteristics of both loading, as well as material fatigue properties can be represented on a log-log plot of load amplitude versus number of cycles. The loading, is represented as a load spectrum, where-as the material properties are presented as Stress-Life curves. Load spectrum curve (a) may, for arguments sake, represent the loading on an automotive component in off-road conditions (high amplitudes, low number of cycles), where-as curve (b) may represent the same component loading under highway loading conditions (low amplitudes, high number of cycles). The two curves, as well as others in between, represent the scatter in loading on a component. Grubisic concludes that to determine the design spectra for the fatigue evaluation of a vehicle component and assembly the following must be regarded:

- The load spectrum must take into account all possible loading conditions, including extreme values during customer usage which would seldom be achieved.

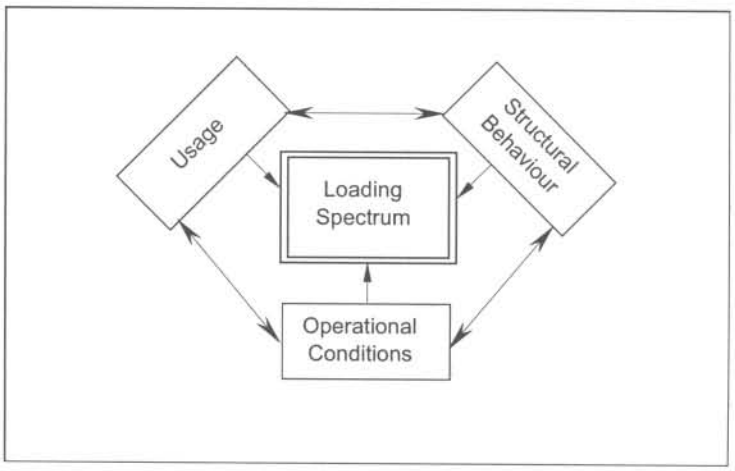

Figure 2.4: Parameters of the loading spectrum

- An appropriate extrapolation of the field measurements can be carried out only if the data for individual loading conditions, originating from the vehicle usage and operational conditions, are separated.

2.2.4 Statistical Domain

Leser et al [23] presents a method to establish fatigue loading histories, using a statistical model. The methods of modelling irregular fatigue loading histories can be divided into two groups, namely counting methods (rainflow etc.) and methods based on correlation theory. The Autoregressive Moving Average (ARMA) model is an example of the statistical correlation theory. The random processes of a ground vehicle travelling on a rough road, are considered to consist of a slowly varying process and a fast varying process. The slow varying process is called the non-stationary mean variation, and the fast varying process is called the stationary random variation. The mean variation is modelled with a Fourier series, while the ARMA model is employed to model the stationary random variation. A concise description of complex loading is achieved, while the overall frequency content and sequential information are statistically preserved.

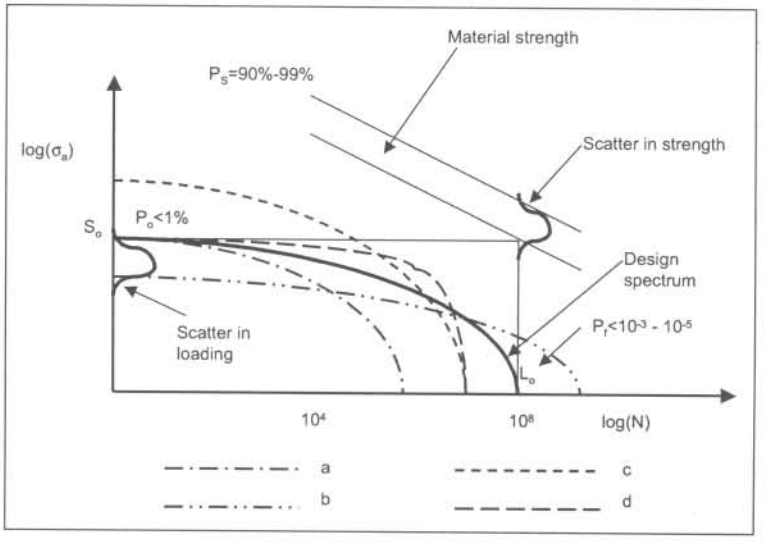

Figure 2.5: Design spectrum of a loading spectrum

2.2.5 Frequency Domain

The frequency domain method of determining the input loads of structure, has become an attractive method on account of the compactness of the data. The time domain stress histories dealt with in engineering can usually not be specified by a formula. The data is represented by a series of values, usually taken at equal time intervals. Time domain data can contain very large amounts of data, that even at this point, where the cost of data space is relatively cheap, can become quite cumbersome to handle. If a structure has to be measured over a long period of time, for instance two years, the use of time domain data can be extremely difficult to store and analyze. Wannenburg [39] employs a method of measuring frequency data in a case study. The frequency domain data is converted to time domain data, to be used in fatigue calculations.

A very important point regarding frequency domain data, is that frequency has no fundamental effect on fatigue life. If a steel cantilever beam is moved up and down between certain limits at a frequency of $10Hz$ and it breaks after 10 000 cycles, a similar beam excited at $1Hz$, will also fail after 10 000 cycles. Time domain data can be stored in the frequency domain by using the

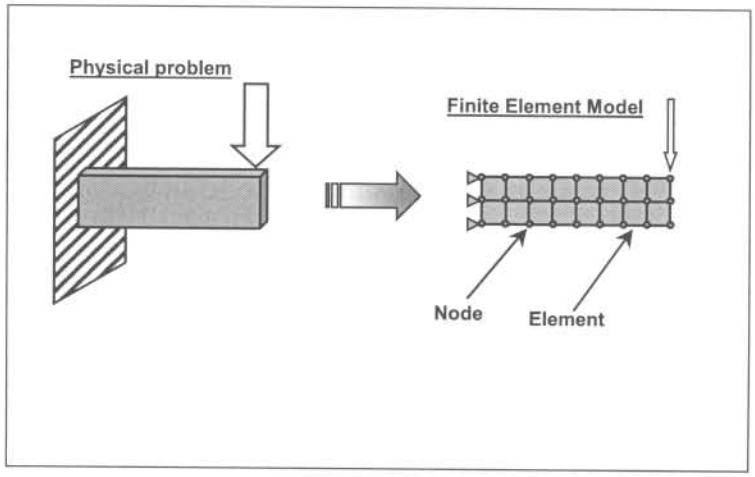

Figure 2.6: Fundamentals of the finite element method

Power Spectral Density (PSD) plot. The PSD format represents the averaged statistical information for each frequency contained in the original time domain data. Using the Fast Fourier Transform (FFT) the ranges ($\Delta\sigma$) are averaged to energies, usually in MPa^2/Hz units, and the number of cycles (n_i) to frequency (Hz). It should therefore be possible to reconstruct a time history from a PSD plot and to carry out a fatigue life prediction. Sherrat [32] explains the method of doing the reconstruction of time domain data, using Inverse Fast Fourier Transform methods. Sherrat mentions the general approach used by Dirlik [13]. The aim of Dirlik's thesis was to produce a general formula predicting the rainflow range distribution from characteristics of the PSD. Random phase angles, in conjunction with statistical methods, were used to create the Dirlik formula. According to Sherrat [32] the agreement between the rainflow ranges, computed by the Dirlik formula, using a PSD plot, and the rainflow ranges computed from time domain data, is excellent. The frequency domain can also be used in the measurement process of vehicles during durability assessments.

2.2.6 Closure

This section discussed the various methods that can be employed to obtain measurements of loads that act on a vehicle structure. The following section discusses the fundamentals of the finite element method (FEM).

2.3 Finite Element Structural Analysis

Finite element procedures are at present widely used in engineering analysis. The procedures are employed extensively in the analysis of structures, heat transfer and fluidflow. Finite element procedures can be employed in virtually every field of engineering analysis. This thesis makes use of the structural capabilities of the finite element method.

2.3.1 Linear Static finite element analysis

The development of the finite element methods for the solution of practical engineering problems began with the advent of the digital computer. The essence of a finite element solution of an engineering problem is that a set of governing algebraic equations is established and solved. By the use of the digital computer, the finite element process could be rendered practical and given general applicability.

The basis of the finite element method for the analysis of solid structures can be summarized in the following steps: The solid structure, representing the real life article, is subdivided in small parts, called *elements*. The elements are assembled through the interconnection at a finite number of points on each element. These points are called *nodes*. The assembly of the elements and nodes is often referred to as a mesh. Within each element we assume a simple general solution to the governing equations. The solution of each element equation is a function of unknown solution values at the nodes. By subdividing the structure in this manner, one can formulate equations for each separate finite element which are then combined to obtain the solution of the

whole physical system [7] (refer to figure 2.6). Equation 2.4 indicates the fundamentals of the finite element method. The stiffness matrix, $[K]$, contains the physical geometrical and material properties of the structure. Vector $\{d\}$ contains the displacements of the structure, while the $\{f\}$ vector is the external load that is applied to the model. The displacements (for each node) are solved for a given mathematical model, contained in $[K]$, and the applied loads in $\{f\}$.

$$[K]\{d\} = \{f\} \tag{2.4}$$

where :

$[K]$ = Stiffness matrix

$\{d\}$ = Node displacement vector

$\{f\}$ = Applied nodal load vector

Figure 2.7 summarizes the process of finite element analysis. The physical problem typically involves an actual structure subjected to certain loads. The idealization of the physical problem to a mathematical model requires certain assumptions that together lead to differential equations governing the mathematical model. The finite element analysis solves this mathematical model. The finite element analysis will solve only the selected (or assumed) mathematical model [2]. Only physical information contained in the mathematical model can be solved. The analysis can therefore be used only to obtain insight into the physical problem considered, because it is impossible to reproduce, even in the most refined mathematical model, all the information present in the real life situation. The choice of an appropriate mathematical model, governed by boundary conditions, geometry, and above all, loads, is therefore of critical importance. Rahman [29] proposes a methodology for the finite element analysis in a systematic fashion with a view to identifying and controlling any error or uncertainty that may be encountered during the analysis process.

The use of non-linear finite element methods does exist, but is seldom used

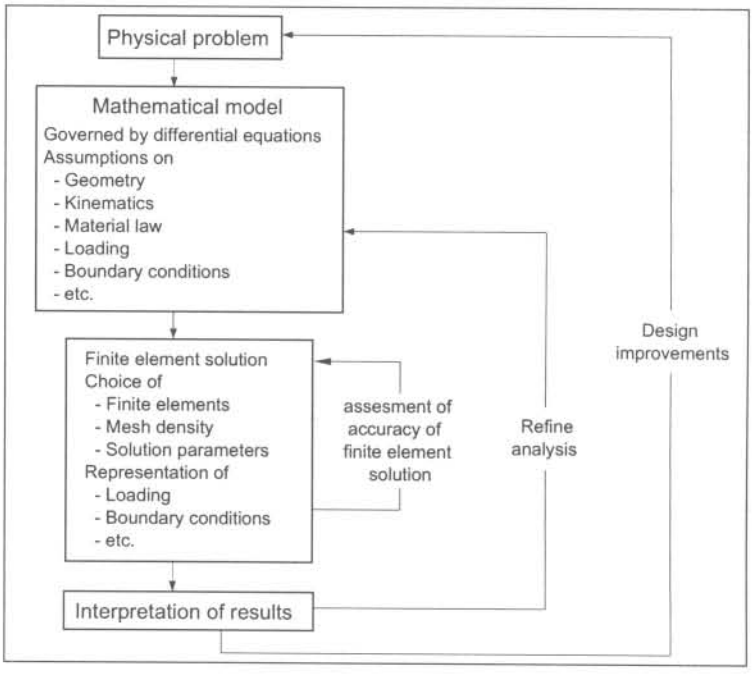

Figure 2.7: The process of finite element analysis

for fatigue analysis. Khatib-Shahidi et al [21] does however make use of a non-linear static analysis. The resulting stresses encountered in the non-linear analysis, according to the paper, are however lower than the yield stress of the material. The most frequently used structural finite element analysis is the linear static analysis. The linear static analysis assumes a linear material behaviour when a load is applied to the structure. A static load, which does not change with time, is applied to the structure in this analysis. In the analysis of structures that would fail by fatigue, the nominal stresses are mostly much lower than the yield strength of the material (otherwise other failure modes would supersede the fatigue mode). The linear static finite element analyses are therefore mostly sufficient.

2.3.2 Linear Dynamic finite element analysis

When a structure is subjected to a load that varies with time, its corresponding response will also vary with time. In a linear static analysis, the loads are assumed to be static, and therefore the response is static and proportional to the structure stiffness and applied loads. If a load is applied at a frequency lower than one third of the frequency of the lowest natural frequency of the structure, the analysis can be done assuming static conditions [7].

However, when the applied loading varies rapidly, the solution techniques must take inertial effects due to damping and material mass in consideration. Several different procedures exist that solve these dynamic analyses. Equation 2.5 is the general formulation of the solution that must be solved during a dynamic analysis. This equation is the set of differential equations of motion in matrix form for the dynamic response of any given structure modelled with a finite number of degrees-of-freedom.

$$\underbrace{[M]\{\ddot{D}\}}_{inertial} + \underbrace{[C]\{\dot{D}\}}_{damping} + \underbrace{[K]\{d\}}_{stiffness} = \{f_t\} \tag{2.5}$$

where :

$[M]$ = Mass matrix
$[C]$ = Damping matrix
$[K]$ = Stiffness matrix
$\{\ddot{D}\}$ = Node acceleration vector
$\{\dot{D}\}$ = Node velocity vector
$\{d\}$ = Node displacement vector
$\{f_t\}$ = Applied time varying nodal load vector

Three basic methods exist with which a structure can be dynamically analysed:

- *Eigenvalue Analysis*: The eigenvalue analysis calculates the natural fre-

quencies of the structure. The eigenvalue problem derives from equation 2.5 after zeroing the damping coefficients and applied forces. The corresponding mode shapes for each frequency can subsequently be calculated.

- *Frequency Response Analysis*: The frequency response analysis calculates the steady state response of a structure that is subjected to harmonic forces at a given frequency. A harmonic load with a frequency equal to the natural frequency will produce infinite displacement responses if no damping is specified. Determining the amount of damping in a structure is a very difficult process. Most structures are however lightly damped, and can be simplified by neglecting the damping, bearing in mind the natural frequencies.

- *Transient Response Analysis*: If the input loading function is not harmonic, but an arbitrary dependent function, a transient response dynamic analysis must be performed. One method to solve a random load is to use a *direct integration method.* Equation 2.5 is solved at discrete time intervals (Δt) apart. The direct integration technique is based on the assumption that displacements, velocities and accelerations within each time interval vary. A second approach to the transient response analysis is the *modal superposition* method. The basis of this approach is an assumption that superposition of the mode shapes corresponding to the lower natural frequencies adequately represents the dynamic response of the structure. The complete response is found by the summation of correct fractions of the low frequency mode shapes.

The linear dynamic analysis for a random input signal is an expensive and difficult finite element method, due to the fact that hundreds of static solutions must be solved. Most literature concerning random load vectors, prefers the use of a static finite element solution. The aim of this thesis is to explain the use of a linear static solution for a random time varying load.

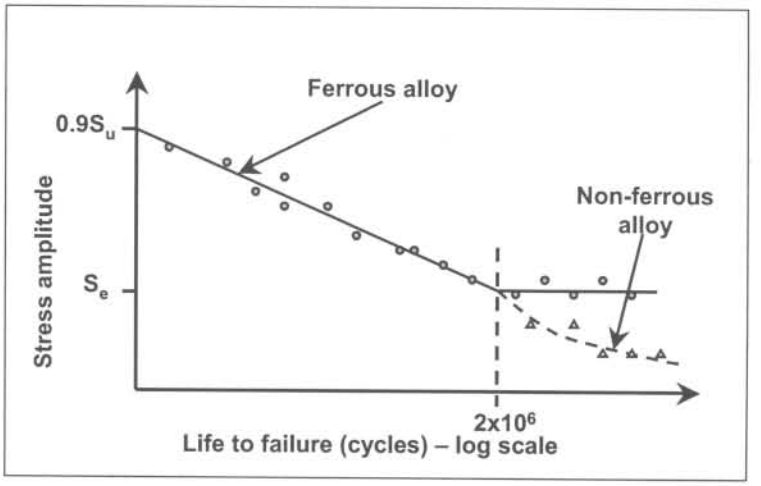

Figure 2.8: The Wöhler or SN curve

2.3.3 Closure

This section explained the fundamentals of the finite element method. Measurements, finite element analyses and fatigue calculations form the building blocks of a *fatigue assessment* of a structure. The combination of these tools enables the engineer to asses a vehicle for fatigue loads. The following section will discuss fundamentals of fatigue and durability calculations.

2.4 Fundamentals of Fatigue and Durability

The load and structural information acquired in accordance with the previous two sections must be analysed, using fatigue principles, to determine the appropriate fatigue damage. This section explains the fundamentals of these theories.

2.4.1 Fatigue analysis

Stress-life

The stress-life (SN) method was the first attempt to understand and quantify metal fatigue. August Wöhler conducted experiments from approximately 1850 to 1875 to establish a safe alternating stress below which failure would not occur. It has since been the standard design method for the past 150 years. The stress-life approach to fatigue life prediction is still widely used in design applications where the applied stress is primarily within the elastic range of the material and the fatigue life of the component is long. The stress-life method does however not work very well for applications where a low-cycle fatigue life is experienced.

The fundamentals of the stress-life approach can be summed up in the Wöhler or SN diagram (refer to [1]). The Wöhler diagram plots stress amplitudes σ_a (alternating stress) versus cycles to fatigue (N). The data for the Wöhler diagram is generated using laboratory tests. Due to the extensive work that has been done in the past 100 years, fatigue data relevant to the stress-life approach is fairly common.

Certain materials, mostly ferrous steels, have a fatigue limit stress (S_e), which is a stress amplitude level below which the material has an 'infinite' life-time. Most nonferrous alloys, for example aluminium, have a SN line with a continuous slope. For *both* these SN curves, a pseudo-endurance limit or fatigue stress is defined at a chosen number of cycles (for example 2×10^6 cycles). It should be noted that certain empirical relationships between the fatigue properties and the monotonic tension and hardness properties have been determined for steel. The fatigue limit stress (S_e) can be related to the ultimate strength (S_u) in the following way: $S_e = 0.5S_u$. A designer can therefore determine the fatigue material properties (of ferrous steel) without doing expensive laboratory tests.

Instead of the graphic approach, a power relationship can be used to estimate the fatigue life of a material (refer to equation 2.6).

$$\sigma_a = C\sigma_f(N)^b \tag{2.6}$$

where :

σ_a = amplitude stress
C = constant relating to the SN – curve (fatigue ductility coefficient)
σ_f = fracture stress
N = number of cycles to failure
b = Basquin's fatigue strenght exponent

In equation 2.6 the constant C represents the value where the SN curve intersects the y-axis of the Wöhler diagram. The exponent b is the gradient of the the SN curve. These two values can be determined using the empirical relationships previously mentioned, or through data derived from test specimens in a laboratory. The constant C is sometimes replaced by the true fracture stress (σ_f). The true fracture stress is an *estimate* of the stress amplitude at either 1 or $\frac{1}{4}$ cycles. The following relationships and definitions are used when discussing alternating stresses. Also refer to figure 2.9.

$$\begin{aligned} \Delta\sigma &= \sigma_{max} - \sigma_{min} &&= \textit{stress range} \\ \sigma_a &= \tfrac{1}{2}(\sigma_{max} - \sigma_{min}) &&= \textit{stress amplitude} \\ \sigma_m &= \tfrac{1}{2}(\sigma_{max} + \sigma_{min}) &&= \textit{mean stress} \end{aligned}$$

Strain-life

The strain-life method was developed in the 1950's, during work that was done to establish the quantified relationships between plastic strain and fatigue life. Early research showed that fatigue damage is dependent on deformation or strain. When a specimen is subjected to low load levels, the stresses and strains are linearly related. However, in the low cycle fatigue domain (cycles $< 10^3$), the cyclic stress-strain response and the material behaviour are best modelled

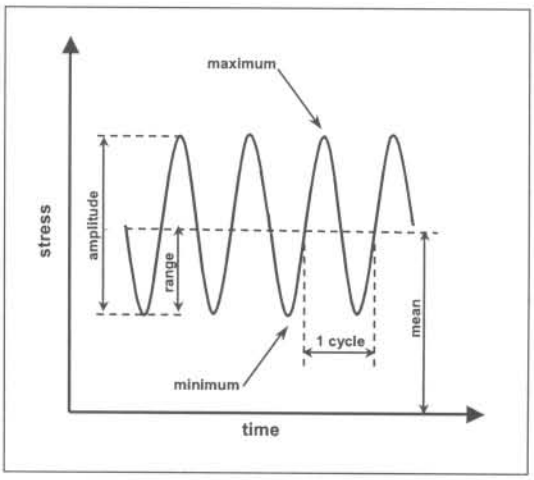

Figure 2.9: Terminology for alternating stress

using strain-life techniques. At long fatigue lives, where the plastic strain is negligible, the stress-life and strain-life approaches are essentially the same. Bannantine [1] explains the fundamentals of the strain-life approach. The strain-life equation (refer to equation 2.7) is used to predict fatigue life, using four empirical constants. A graphical representation of equation 2.7 illustrates how the strain-life methodology approaches the stress-life approach at low amplitude loading conditions (refer to figure 2.10).

$$\frac{\Delta\epsilon_p}{2} = \underbrace{\frac{\sigma'_f}{E}(2N_f)^b}_{elastic} + \underbrace{\epsilon'_f(2N_f)^c}_{plastic} \tag{2.7}$$

where :

σ'_f = fatigue strenght coefficient

$\Delta\epsilon_p/2$ = plastic strain amplitude

$2N_f$ = number of reversals to failure

b = Basquin's fatigue strenght exponent

E = Young's elasticity modulus

ϵ'_f = fatigue ductility coefficient

c = fatigue ductility exponent

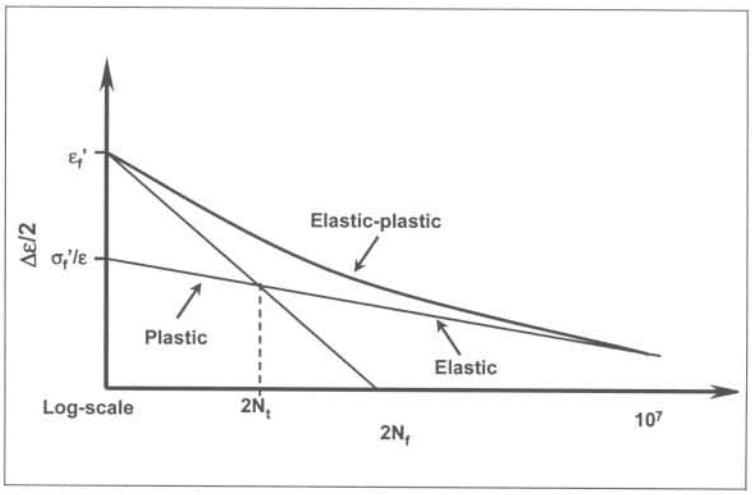

Figure 2.10: Graphical representation of the strain-life equation

Neuber's rule can be used in the strain-life approach to determine the notch root stresses and strains (local stresses and strains) at stress concentrations, for instance a hole in a plate (refer to equation 2.8). Conle et. al [10] make use of the stress-strain behaviour of a material to measure fatigue life. Conle reports that the uni-axial parameter and equivalent stress parameters does not work well under multi-axial conditions. The use of strain-life procedures is therefore more adequate for complex multi-axial loading conditions.

$$K_t = \sqrt{K_\sigma K_\epsilon} \tag{2.8}$$

where :

K_t = theoretical stress concentration factor

K_σ = local stress concentration factor

K_ϵ = local strain concentration factor

Multi-axial fatigue theory is still the subject of ongoing research. The

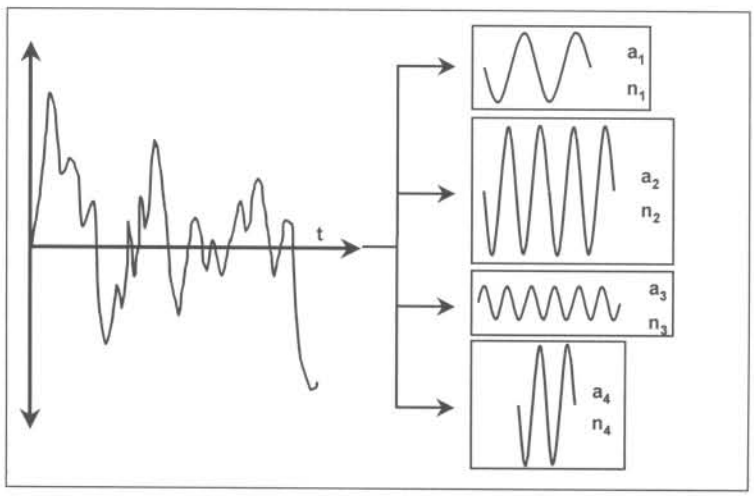

Figure 2.11: Primary objective of cycle counting

strain-life approach is mostly applicable to the low cycle fatigue domain. Vehicle structures are however designed to withstand many millions of load cycles. For these reasons, the stress-life approach was the preferable choice for durability analyses in this thesis.

Fracture Mechanics

Fracture mechanics approaches are used to estimate the crack propagation life due to fatigue loads.

These methods require that an initial crack size be known or assumed. Some components with imperfections, such as welding porosities, inclusions etc., have an initial crack size that can be determined. The assumed initial crack size may be determined also by the requirements of the designer. The linear elastic fracture mechanics approach (LEFM) is the most commonly used method in this field.

The stress intensity factor, K, is used to relate the local stress magnitude at the crack tip, using remote nominal stresses. Refer to equation 2.9. This factor depends on loading, crack size, crack shape and geometric boundaries.

$$K = f(g)\sigma_n\sqrt{\pi a} \tag{2.9}$$

where :

σ_n = remote nominal stress applied to the component

a = crack length

$f(g)$ = correction factor (depends on geometry, loading and crack shape)

The LEFM approach aims to calculate the crack growth in a component. The most current applications of the LEFM concepts describe this crack growth in the region where the crack growth is stable. The Paris equation (eq. 2.10) is the most widely accepted curve fit for this region.

$$\frac{da}{dN} = C(\Delta K)^m \tag{2.10}$$

where :

C = material constant

m = material constant

ΔK = $K_{max} - K_{min}$ (stress intensity range)

Multi-axial loading

Engineering components are often subjected to complex loading conditions. A component, for example a vehicle's rear axle, is subjected to a combination of bending and torsion. Complex stress states, stress states in which the three principal stresses are non-proportional and/or whose directions change during a loading cycle, very often occur at geometric discontinuities, such as notches. However, metal fatigue due to this phenomenon is still the subject of ongoing basic research [1]. Although there has been no consensus yet about the best approach among the various methods proposed, the need to use multi-axial

fatigue methods for non-proportional loading conditions has been recognized by the significant improvement in fatigue life prediction accuracy these analyses yield over traditional uniaxial methods [8]. Many different parameters have been suggested to correlate loading and fatigue life of multi-axial stressed components. All of these parameters can be subsumed under the term *critical plane approach*. The critical plane approach models initiation and growth of small fatigue cracks by analyzing different potential crack directions at one structural location, selecting the most damaging direction as crack initiation plane [14]. Chu [8] describes a procedure to solve multi-axial fatigue problems using (a) a three-dimensional cyclic stress-strain model, (b) the critical plane approach, (c) a bi-axial damage criterion for better fatigue damage evaluation and (d) a multi-axial Neuber equivalencing technique used to estimate multi-axial stress and strain history of plastically deformed notch areas.

Due to the limited amount of experience at present, Dreßler et. al. [14] therefore proposes a procedure that not necessarily predicts fatigue life very accurately, but rather uses numerical procedures to evaluate different design alternatives. Due to the fact that multi-axial fatigue is still the subject of ongoing research, and has not yet been resolved, the testing of components for this type of loading is still essential.

2.4.2 Cycle counting and Damage accumulation

Cycle counting

To predict the fatigue life of a component that is subjected to a *random* load, the variable time history must be reduced from a complex history to a number of events that can be compared to available *amplitude* history (refer to figure 2.11). This process of reducing the complex load history is termed *cycle counting* [1]. The proper way of counting the loads is the rainflow cycle counting method. Matsuishi and Endo first proposed it in 1969 [25]. A number of variations of the rainflow cycle counting method has been proposed and it has subsequently been standardized by the ASTM, SAE and AFNOR [14]. The

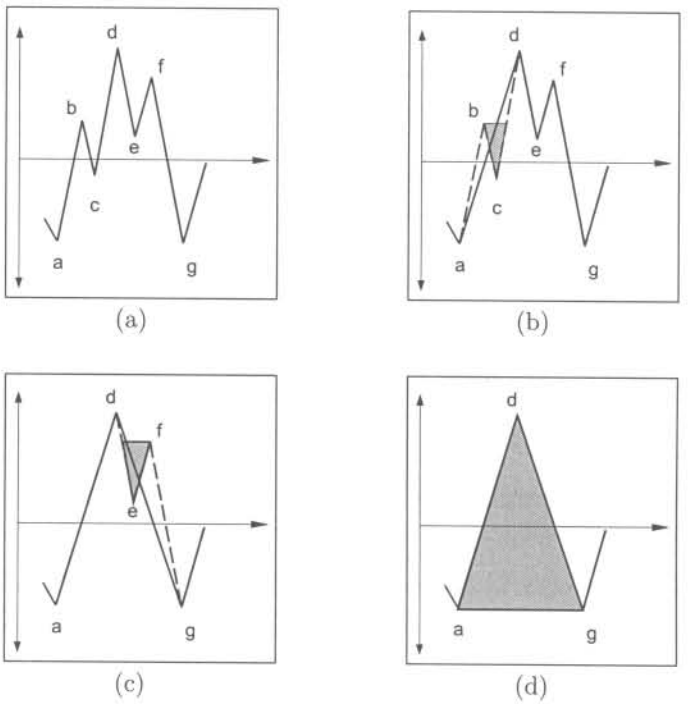

Figure 2.12: Rainflow counting: ASTM standard

ASTM standard for rainflow counting (also called range-pair-range counting) is shown in figure 2.12. The recommended practice is also called the four point method. It should be noted that various cycle counting techniques are equally well regarded.

The Markov matrix is used to store the data that is obtained from the rainflow matrix [12]. The Markov matrix stores the total number of hysteresis loops (or cycles) for all the rain flow ranges (refer to figure 2.13). In this figure, the cycle counting method has counted four cycles that go *from* stress level 70 *to* stress level 10. Dreßler et al [14] also describes methods to do rainflow counting on multi-axial loading processes, as well as rainflow reconstruction. Olagnon [26] discusses the practical implementation of the statistical properties of the rainflow counting method established by Rychlik. Sherrat [32] describes various methods when using the rainflow counting method with frequency domain data. This method makes use of computer modelling of the inverse

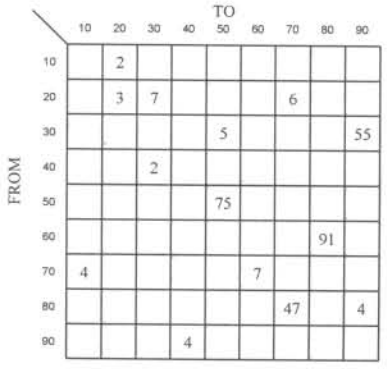

Figure 2.13: An example of a Markov matrix

Fourier transform first, and then the establishment of a theoretical link between the Power Spectral Density diagrams and the rainflow ranges. However, this method is still a topic of research. Dietz [12] makes use of another method to do cycle counting. His method maps an equivalent stochastic load signal to an equivalent harmonic process, using *cumulative frequency distributions*. The rainflow counting (or range-pair-range) method described in figure 2.12 is used in this thesis to analyze the measured data.

Damage accumulation

The data contained in the Markov matrix can be used to calculate the damage that the loads cause. There are two distinctly different approaches used when dealing with cumulative fatigue damage during the initiation period and the propagation period. During the crack propagation period, the damage can be related to a measurable crack length. However, during the initiation stages, the damage of the component can be detected only in a highly controlled laboratory environment (slip bands, micro-cracks etc.). Because of the difficulty of measuring the damage during the initiation stage, the damage summing methods are *empirical* in nature [1]. The linear damage rule was first proposed by Palmgren in 1924 and then further developed by Miner in 1945. The linear

damage rule is usually referred to as Miner's rule in the literature.

The damage fraction, D_i, is defined as the fraction of life used up by an events or a series of events (refer to equation 2.11). The number of cycles counted by the rainflow counting method is n_i, at a stress level S. The number of fatigue life in cycles, N_i, is obtained from the Wöhler diagram (figure 2.8) at stress level S.

$$D_i = \frac{n_i}{N_i} \tag{2.11}$$

where :

D_i = damage fraction

n_i = number of load cycles at stress level S

N_i = number cycles to failure for stress level S

The total damage, D, is the sum of all the damage fractions (refer to equation 2.12). Failure of the component is assumed to occur when the summation of damage fractions equals one (1). Considerable test data has been generated in an attempt to verify Miner's rule. Most of the results tend to fall between 0.5 and 2.0. In most cases the average value is close to Miner's proposed value of one. Non-linear damage theories have been proposed which attempt to overcome the shortcomings of Miner's rule. Equation 2.13 shows an example of a nonlinear equation. However, nonlinear damage rules do not give significantly more reliable predictions. For most situations, where there is a pseudo-random load history, Miner's rule is adequate.

$$D = \sum_{i=1}^{n} \left(\frac{n_i}{N_i} \right) \tag{2.12}$$

$$D_i = \left(\frac{n_i}{N_i} \right)^P \tag{2.13}$$

Various damages, calculated for various measured loads using equation 2.12,

can be added to give a more realistic damage regarding the total life cycle of a vehicle. This is an important concept due to the cost involved in the measurement of loads on a vehicle. Various articles have been published that address this issue. Beamgard et al [3] reports a method of establishing durability test objectives which accurately reflect field usage. Three basic inputs are required for this procedure:

1. Field Usage Data: This input defines the distribution of field usage in terms of cargo and passenger loading, mileage over various types of terrain, etc. This data is obtained from interviews of vehicle owners.

2. Field Fatigue Damage Data: This data is obtained from a fatigue damage analysis of road-load-strain data acquired during a large sampling of public roads.

3. Durability Fatigue Damage Data: This input defines the fatigue damage incurred in the proving ground durability events.

Inputs (1) and (2) are used to calculate the damage incurred by each customer. This data is used to determine the distribution of the customer damage. Input (3) is consequently used to match the customer damage distribution with an equivalent durability damage. It should be noted that the inputs obtained for this analysis took extensive research that was done over a three year period. This approach is therefore mostly applicable to large corporations with a large number of vehicles (and customers) that can be evaluated. Slavik and Wannenburg [34] also employs a similar method to evaluated vehicle failures due to fatigue. The article reports interesting procedures, using statistical methods, to predict the failure of components of vehicles. The same three basic inputs mentioned by Beamgard are used in the analysis. The obtained input data is also converted to damage values that represent the various roads and users. These damage values are subsequently manipulated using statistical methods and Monte Carlo simulations to obtain realistic damage values that can be used. Wannenburg and Slavik used the damage values to predict failures in the field, while Beamgard used the damage calculations to calibrate durability

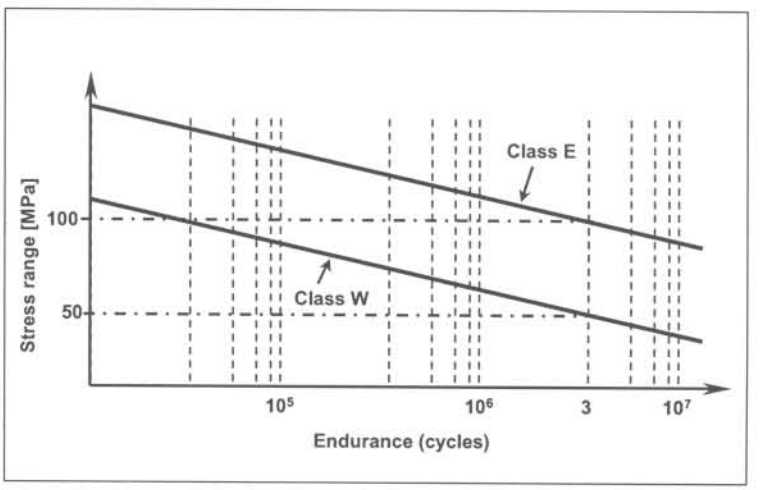

Figure 2.14: BS fatigue SN curves for welds

test tracks as well as to identify potential areas where components must be redesigned.

2.4.3 Welds

Welded joints

The fatigue life of a welded joint is almost always lower than the fatigue life of the parent material. The fatigue evaluation of welded joints in vehicles is therefore of utmost importance. Many codes exist that address the fatigue design of components (see references [40], [15] and [9]). The fatigue codes describe different classes of welds. The class of weld determines the fatigue life of the welded joint. For example, according to the BS steel-code [40], a weld in class W would have a fatigue life of 3×10^6 cycles if a load with a stress range of 50 MPa is applied. A weld in class E could however withstand a stress range of 100 MPa resulting in the same fatigue life (refer to figure 2.14). Gurney [18] delivered various publications regarding the fatigue design of welds. The use of fatigue design codes is consequently explained, making use of Gurney's article [18]. The fatigue design codes make use of Stress-Life (SN) diagram. The fatigue weld SN-diagram looks, and is, very similar to the Wöhler curve

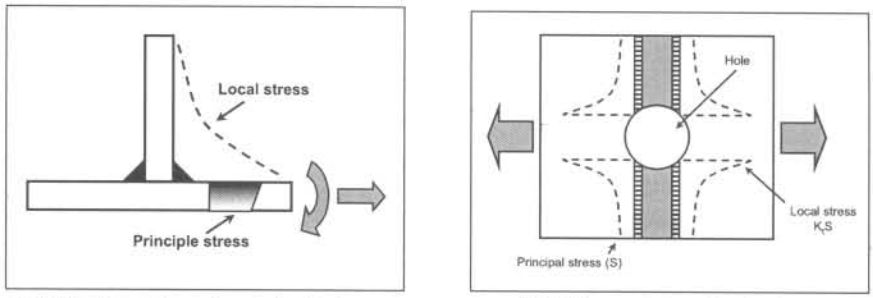

(a) Explanation of nominal stress (b) Stress intensity factor

Figure 2.15: Weld stress interpretation

introduced in the stress-life methodology. The reader should however note that theory of these curves is closely tied in with fracture mechanics. The assumption is made that the whole of the fatigue life of a welded joint consists of the propagation of a pre-existing small defect. The ECCS code [15] considers all of the weld classes to have slope (m) of -3. The BS-code does however have 2 classes with less steep slopes, but essentially all the other joint classes also have a SN-slope of -3. This is the same as m exponent used in the Paris equation (2.10) to calculate fatigue crack growth (refer to figure 2.14).

The stress range stresses referred to in figure 2.14 are to be considered as nominal stresses. Thus, the combined effect of bending, shear, etc. should be considered. The design stresses quoted can therefore be regarded as the nominal stresses adjacent to the detail under considerations, usually the parent material at the weld toe. The codes make the assumption that, in an as-welded structure, high tensile residual stresses are liable to exist as points of fatigue crack formation. However, stresses at weld joints that are situated in regions of geometric stress concentrations, must be factored to take the higher stresses into account. If a nominal stress (S) is applied to a T-joint with a hole in, the factored nominal stress, K_tS, must be considered using the stress curves (refer to figure 2.15(b)).

Jones et al [20] discusses the method of using finite element models to analyze the fatigue failures of welds on a structure. The paper makes use of the British Standards codes [40], combined with the above mentioned procedures.

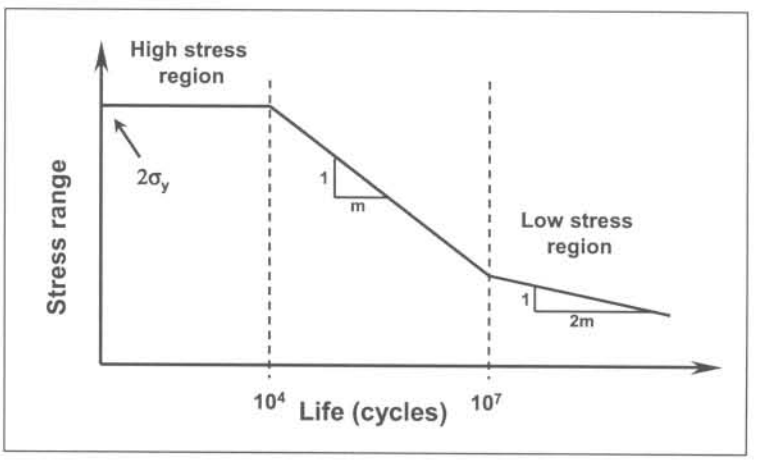

Figure 2.16: A hot-spot SN curve

Stephens [37] also makes use of the above mentioned method. However, Stephens' paper also makes use of the United Kingdom Department of Energy's research on offshore structural welds (UKOSRP) [30]. The research uses the 'hot-spot' stresses on and near the weld to define an additional fatigue life region (refer to figure 2.16 [38]).

Spot welds

Rui and Borsos [31] describes a method for life prediction of multi-spot-welded structures. The fatigue strength of spot welds in a multi-spot-welded structures is one of the key issues of concern for achieving structural durability and optimum design in the vehicle industry. Three failure mechanism criteria have been proposed to predict spot weld failures: (a) load range criteria, (b) strain range criteria and (c) stress intensity factor (K) criteria. Although the load range criteria is the easiest method to use, the method requires adequate experimental data. The other two criteria can however not be used in conjunction with the *simplified* finite element methods. A spot weld can be modelled in detail, using solid elements to connect the two plates that are spot welded, though this method is impractical if thousands of spot welds occur on a vehicle. The accepted method of modelling a spot weld is the use of a

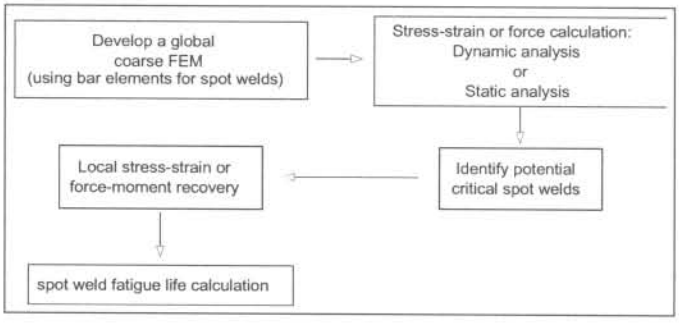

Figure 2.17: A flow chart of spot-weld fatigue life prediction

bar element[1]. Fatigue life calculations can however not be done on the bar element itself. Rather, the 'global' stresses or strains, typically two times the diameter of the spot weld, away from the centre of the spot weld is used. The general methodology of analyzing a multi-spot-welded structure is shown in figure 2.17.

Another method to address the problem of life prediction of shear spot welds is through the use of fracture mechanics. Smith and Cooper [35] noted that a spot weld could be considered to be a circular solid surrounded by a deep circumferential crack, which, when loaded in a combination of Mode I and Mode II, would grow a branch crack in the direction of maximum local Mode I. The forces (and moments) that the bar element experiences are used to calculate the structural or nominal stresses in the weld nugget. These stresses can then be used to calculate the fatigue strength of the spot-weld [24].

2.4.4 Closure

This section discussed the fundamentals of fatigue calculations. The previous three sections presented the building blocks or tools of a fatigue assessment. The combination of measurements, FE analysis and fatigue calculations, enables an engineer to asses a structure for fatigue loads. The following section discusses various strategies developed, using the previously mentioned tools, to asses structures subjected to fatigue loads.

[1] a bar element is structural finite element use to represent a beam

2.5 Integration of Measurements and Analysis

This section provides a few examples of techniques that have been developed to determine a fatigue damage prediction. These strategies incorporate the various methods explained in the previous sections to determine a solution to a structural fatigue problem.

2.5.1 Remote Parameter Analysis

Poutney and Dakin [28] describes a method to integrate finite element analysis and simulation or road test data for durability life prediction. The method was termed the Remote Parameter Analysis (RPA) method. Loads that are applied to automotive components are usually very difficult to determine. The heart of the RPA method is the ability to back-calculate all the free-body component forces, by making use of remotely measured parameters, usually strain. The Remote Parameter Analysis provides the following solution to the determination of input loading:

1. Develop a free body diagram of the component.

2. Build a finite element model. Constraints and unit loads are applied to the model in accordance with the free body diagram determined in step 1.

3. Determine the so-called 'Load2Gauge' matrix at stress concentration areas. This matrix shows direct relationship between the applied unit loads and the resulting stresses/strains on the finite element model.

4. The finite element model is now verified by selecting strain gauge positions on the component (using the finite element results). The component is then tested with known loads, relating to the finite element model, and the stresses/strains are measured. If needed, the finite element model is then modified to achieve a high confidence level.

5. Record in-service strains on a prototype vehicle.

6. The 'Load2Gauge' matrix is used to convert the recorded in-service strains to input loads as a function of time.

7. The most damaging load histories are selected. These loads are then used to calculate stresses and strains, using the 'Load2Gauge' matrix, without performing a finite element analysis. The resulting information is then used to perform durability calculations on the component structure.

Poutney describes a methodology to design a complex, fatigue loaded structure, using the finite element method as well as actual in-service strain measurements. However, the post-processing of the fatigue data (derived from the calculated input loads) could be tedious work, as well as difficult to evaluate.

2.5.2 Body-structure durability analysis

Kuo and Kelkar [22] describes a method developed by Ford engineers to predict structural life of a vehicle before prototypes are built. The method employed by Kuo and Kelkar is very similar to the Remote Parameter Analysis method described by Poutney (also a Ford engineer). The methodology follows the following four steps:

1. Identify relative stress sensitivity, using a finite element model and unit loads.

2. Identify critical load paths.

3. Identify critical road events.

4. Compute fatigue life.

Kuo and Kelkar does however use its method on a full body system, rather than on components taken out of the vehicle. The difficulty of determining the input loading and boundary conditions on a cut-out component is therefore eliminated.

2.5.3 Durability testing

A test spectrum must be different in comparison to the design spectrum due to the demands for a short test time and an economical test procedure. Grubisic [17] also proposed various methods to determine test spectrums. The tests of components should, as far as possible, be accelerated and to some extent simplified (refer to figure 2.4). Curves c and d indicate various load spectrums that can be implemented on a vehicle structure. The following general conditions must be regarded:

- Tests should be accelerated by adjustment of the load spectrum in only the medium and high load levels and omission of non-damaging high-cycle, low-intensity loads, predominantly originating from operational conditions during straight driving over smooth roads. The acceleration by increasing spectrum maximum loads should be avoided.
- It is of decisive importance that the deformations of tested components in a test facility correspond to the deformations under service loading conditions. Adjustments of the test loading must be approved by calibration.
- To meet reliability requirements, several durability tests should be carried out. Using a 'risk-factor', based on a statistical approach, the test requirements could be determined.

2.5.4 Computational fatigue life prediction

Stephens et al [37] illustrates a variable amplitude computational fatigue life prediction method for the use of the ground vehicle industry. This method is especially useful in the prototype iteration/optimization design stage of a vehicle, and can be used with welded or non-welded components. The welded components were evaluated using the hot-spot stress approach developed for off-shore structures (see sub-section 2.4.3). For non-welded notched components, the method incorporates the local notch strain approach. The loads

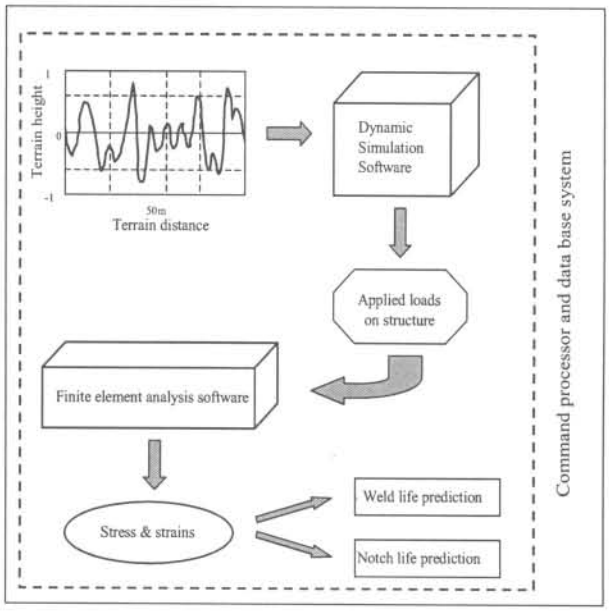

Figure 2.18: Computational fatigue life prediction process

on the vehicle structure were determined using a dynamic simulation software package (DADS). A vehicle terrain profile was selected and used as input to the dynamic simulation software. The resulting forces are therefore calculated using rigid body dynamics and flexible body dynamics. A finite element analysis program (ANSYS) was used to determine stresses and strains using the loads generated by the dynamic simulation software. The resulting stresses and strains are then used to calculated fatigue damage, using either the weld or non-weld methodology. Rainflow counting and linear damage accumulation along with specific material or weld classification properties are incorporated. The interactions between the various calculation phases are managed by a database and command processor that accumulates information, launches application software (like DADS and ANSYS) and stores the resulting data. This software enables the design engineer accurately to control the various processes and resulting data that is generated. Figure 2.18 illustrates the basic principles of the methodology developed by Stephens et al.

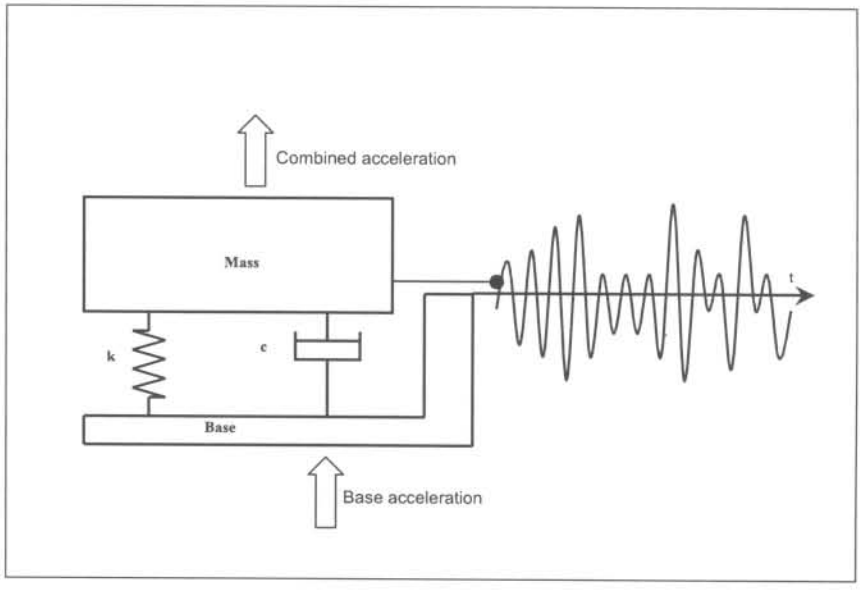

Figure 2.19: Principal sketch of a shock response spectrum

The technique described by Stephens can be very useful during the initial development stages of a vehicle where very little is known about the fatigue loads. The design engineer can acquire a good intuition of the performance of the structure. However, the article does not compare the loads and resulting durability predictions with real life results. As previously mentioned in section 2.2.2, dynamic simulations are still relatively unreliable in determining accurate, realistic random dynamic fatigue loads for ground vehicle structures.

2.5.5 Fatigue assessment through response spectrum methods

Olofsson et al [27] published an exciting paper discussing a methodology to determine fatigue damage caused due to dynamic vibrations. A road vehicle experiences mechanical vibrations due to road surface irregularities. These vibrations may lead to mechanical damage of at least two kinds: (a) the ultimate strength is exceeded as a result of an isolated shock, and (b) fatigue in

the material caused by a large number of load cycles. Olofsson proposes that a Shock Response Spectrum (SRS) analysis could be the appropriate method. The SRS is constructed in the following way. The vibration to be described is theoretically applied to a number of single degree of freedom systems. The maximum response for each system is obtained and then defined as the Shock Response for the frequency and damping factor (see figure 2.19). The more likely reason for mechanical damage to a road vehicle is fatigue damage caused by a large number of cycles. Olofsson describes the Fatigue-Damage Response Spectrum (FDRS) analysis to establish a test sequence for the analysis of structures. The FDRS analysis is carried out in the following steps.

1. From measured acceleration data, the response is obtained from objects with different dynamic properties, modelled with single degree of freedom mechanical systems. This can be done by using fast-Fourier transformations (FFT). The result is a number of response time histories, one for each eigenfrequency or damping factor.

2. From each response time history, the resulting fatigue damage is determined. This is accomplished by combining a stress level count with material properties (Wöhler curve) using Miner's law. The result is a damage for each combination of dynamic properties.

3. The Fatigue-Damage Response Spectrum is constructed as a diagram showing the fatigue-damage measure as a function of eigenfrequency. If damping factors are used it will contain one curve for each damping factor (refer to figure 2.20).

2.5.6 Establishment of input loading for fatigue load structures

Wannenburg [39] published a doctoral thesis regarding the establishment of the fatigue loads that affect transport and vehicle structures. The author aims

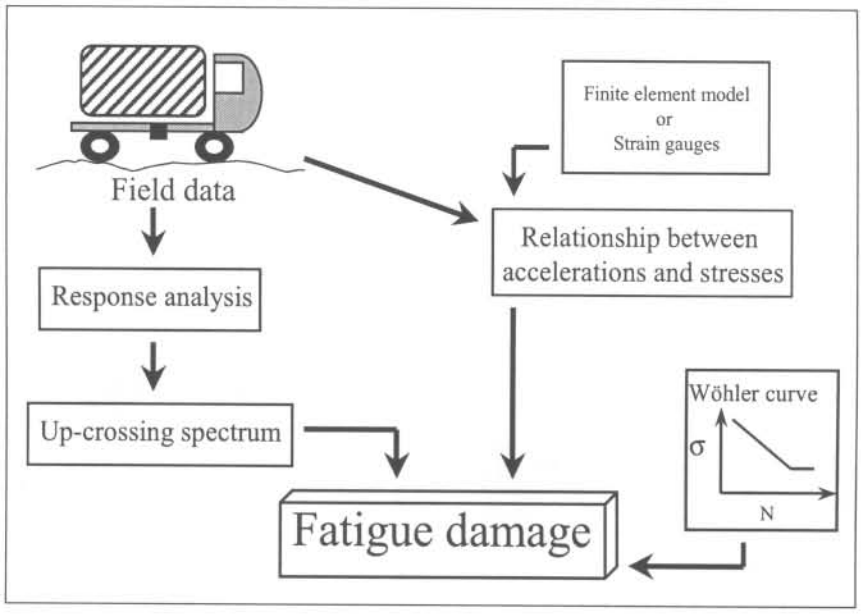

Figure 2.20: Principles of the Fatigue-Damage Response Spectrum method

to develop a Grand Unified Theory (GUT) for fatigue assessment. Wannenburg argues that defective structural design is caused mostly by insufficient knowledge regarding the input of fatigue loads (also refer to Dreßler [14]). Wannenburg's Grand Unified Theory can best be summed up by means of figure 2.21[2]. The left part of the flowchart illustrates the various methods employed by the author to obtain initial input loading. The centre of the flowchart shows the various methodologies developed by the author to process the initial input loads into a well-defined fatigue load. The right part illustrates how the fatigue load can be used for various assessment techniques, for instance design loads, failure prediction and test requirements.

[2]With permission: J Wannenburg

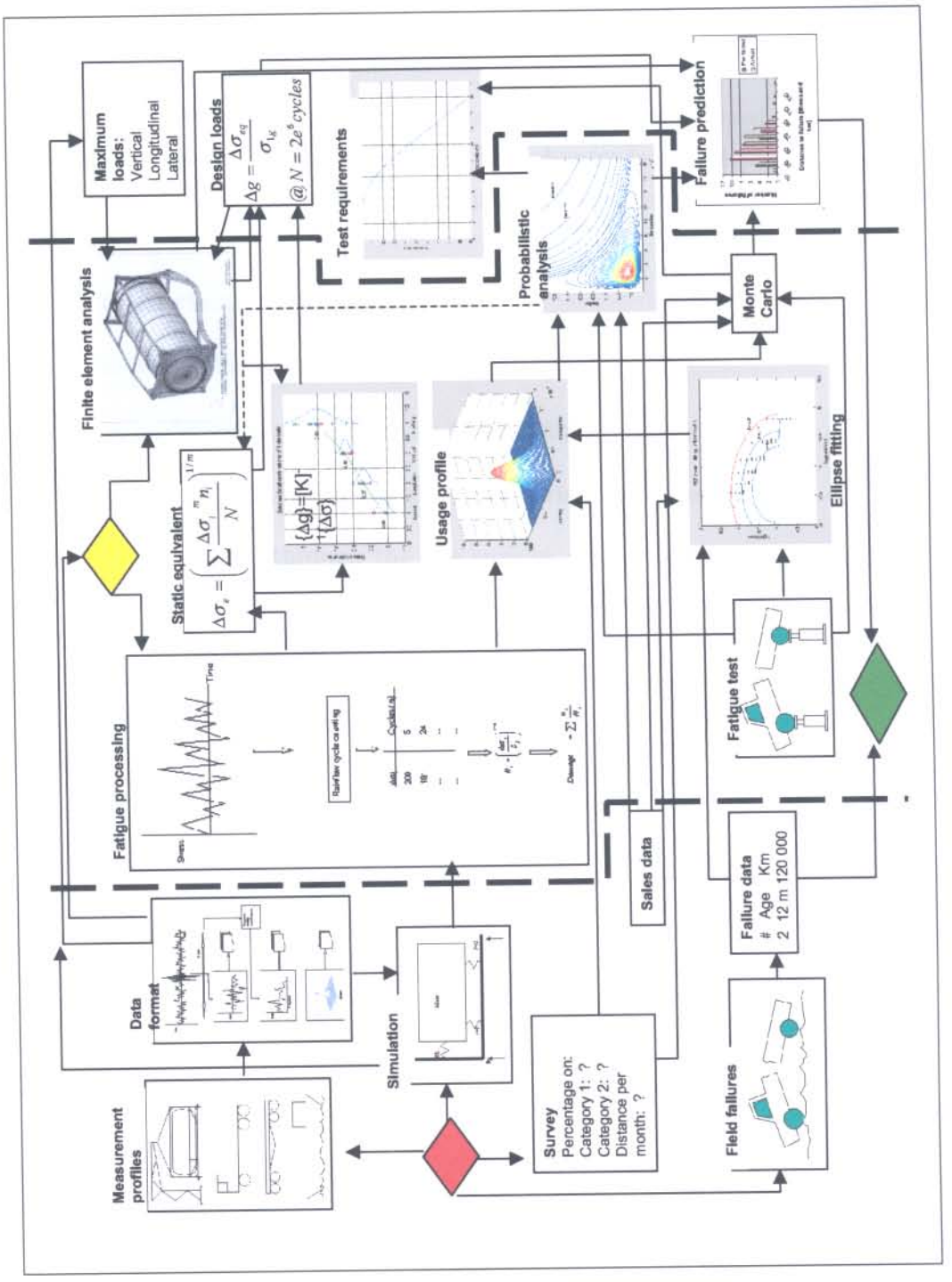

Figure 2.21: Wannenburg's Grand Unified Theory

2.6 Closure

This chapter presented the current theories and practices used by engineers in solving structural fatigue problems. The chapter is sub-divided in sections that follow the various stages of solving a fatigue damage problem. These stages are:

- the determination of input loading.
- the use of finite element structural analysis.
- the fundamentals of fatigue and durability.
- the integration of measurements and various analyses.

This thesis explains, through the use various case-studies, the methodology of the Fatigue Static Equivalent Load (FESL) strategy. The FESL method is very similar to the RPA method that was mentioned previously. The FESL method does have the advantage of simplifying a complex load time history into a *single* load. The following chapter will present a formulation of the Fatigue Equivalent Static Load methodology.

Chapter 3

FORMULATION

3.1 Scope

The previous chapter discussed the various methods and theories practised by engineers to perform structural fatigue evaluations. This chapter will formulate and present the Fatigue Equivalent Static Load (FESL) methodology. Central to this chapter is figure 3.1. Figure 3.1 aims graphically to present the methodology of the chapter.

3.1.1 Determination of input loads

The fatigue equivalent static load method starts with obtaining the input loads that cause fatigue damage to a structure. The case-studies presented in this thesis exclusively used strain gauge and acceleration measurements. Various other techniques can also be used. Refer to Chapter 2, section 2.2 (also see Wannenburg [39]).

Irrespective of the method used to obtain the input loads, the quantities needed for the following step are either strains or loads that can be used ultimately to calculate damage.

3.1.2 Fatigue calculations

Stress conversion

The data obtained from the previous exercise is now used to calculate a *relative damage*. If strains were measured, the data must be converted to stress data. This can be done using either equations 2.1-2.3 or equation 3.1, depending on the strain gauge configuration. Stresses can also obtained be using other methods, for instance dynamic simulations or conversion of frequency domain data. The case-study of the large bus-bracket, made use of the measurement of the input forces. These forces were converted to stresses using laboratory calibration, as well as finite element analysis calibration.

$$\sigma(t) = E\epsilon \tag{3.1}$$

Cycle counting

The stresses obtained from the conversion process are now further refined using the rainflow cycle counting technique. Please refer to sub-section 2.4.2, page 26 for a detailed explanation. The result of the cycle counting process is stress ranges ($\Delta\sigma_i$) and the number of cycles (n_i).

Relative damage

The relative damage of the measurements is now calculated using the stress ranges and cycles ($\Delta\sigma_i$, n_i). The term *relative* is used because generic material properties ($\Delta\sigma_f$, b) are used in equation 3.2. Equation 3.2 and equation 3.3 are used to calculate the damage. The *relative damage* calculated will be used in the next step to calculate the equivalent stress.

$$N_i = \left(\frac{\Delta\sigma_i}{\sigma_f}\right)^{\frac{1}{b}} \tag{3.2}$$

$$D_r = \sum_{i=1}^{n} \frac{n_i}{N_i} \tag{3.3}$$

Equivalent stress

The previous step calculated a relative damage (D_r) using the measured input data. The relative damage can now be processed further to obtain the total damage (D_{tot}) that the structure would experience during its lifetime. Again, various methods can be employed to obtain the total damage, for example questionnaires to determine the usage of the vehicle combined with a statistical analysis (see Wannenburg [39]). Irrespective of the methods employed, a total damage is now used to calculate the equivalent stress that would cause the total damage. The methodology will now be explained. The stress-life equation 3.2 is modified to equation 3.4.

$$N_{eqv} = \left(\frac{\Delta\sigma_{eqv}}{\sigma_f}\right)^{\frac{1}{b}} \tag{3.4}$$

Miner's damage equation can be modified to incorporate the *equivalent number of cycles* (N_{eqv}) resulting from the equivalent fatigue stress ($\Delta\sigma_{eqv}$). The number of cycles of the 'measured' equivalent stress (n_{eqv}) is selected (almost) arbitrarily. Most of the welding codes define an infinite life-time at 2×10^6 cycles. Weld categories, as well as mother material, are usually also defined relative to this life-time. Therefore: $n_{eqv} = 2 \times 10^6$.

$$D_{eqv} = \frac{n_{eqv}}{N_{eqv}} \tag{3.5}$$

The equivalent damage (D_{eqv}) is now set equal to the total damage that the structure would endure during its life-time (D_{tot}). This total damage is therefore equal to an amplitude loading of $\Delta\sigma_{eqv}$ repeated 2×10^6 times, and was calculated using the measurement data. It could mean that the vehicle structure can travel 750 000 km during which it will bend 20 million times at different amplitudes. The accumulated damage would be equal to an amplitude loading of $\Delta\sigma_{eqv}$ repeated 2×10^6 times. This all depends on the way that the total damage (D_{tot}) was calculated, using the relative damage (D_r).

Substituting equation 3.4 into equation 3.5 results in equation 3.6.

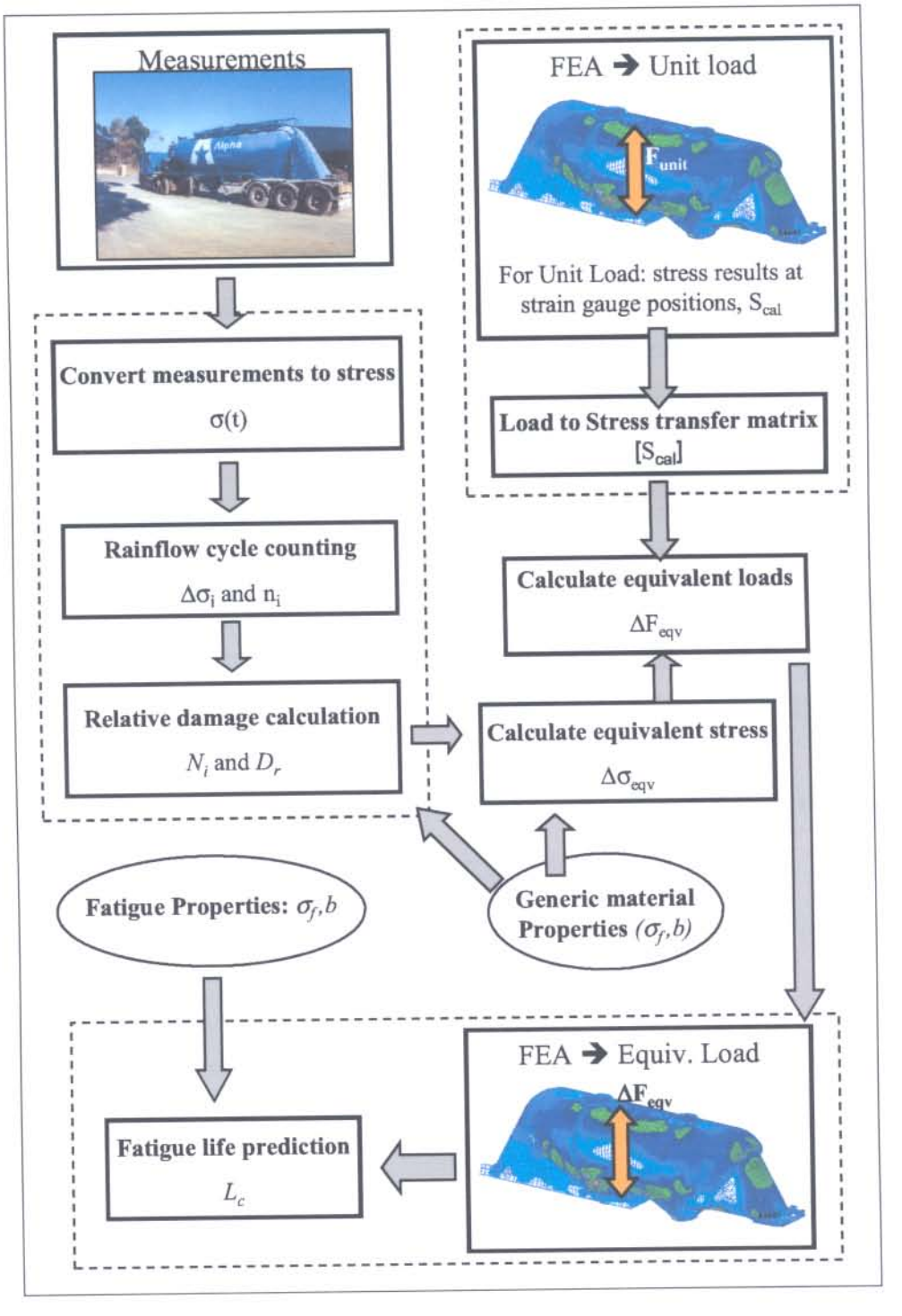

Figure 3.1: Fatigue equivalent static load

$$\Delta\sigma_{eqv} = \left(\frac{n_{eqv}}{D_{tot}}\right)^{b} \times \sigma_f \tag{3.6}$$

Fatigue equivalent static load

The finite element model is now used in this part of the process. The finite element model of the structure is subjected to a unit load (F_{unit}). The finite element analysis determines the stresses that the structure will experience because of the unit load. A *calibration* stress (ΔS_{cal}) can now be obtained at *the exact position where strain measurements were recorded.* An equivalent fatigue static load (ΔF_{eqv}) can now be determined using equation 3.7.

$$\Delta F_{eqv} = F_{unit} \times \frac{\Delta\sigma_{eqv}}{S_{cal}} \tag{3.7}$$

3.1.3 Assessment

The finite element model can now be analysed using the *fatigue equivalent static load.* The process of assessing the structure for fatigue damage can be summarized as follows:

- Analyze the finite element model, using the fatigue equivalent static load.
- Determine the highly stressed areas (*critical positions*).
- Determine the number of cycles to failure (N_c) for each critical position. Refer to equation 3.8.
- Calculate the damage (D_c) that the critical position will experience. Refer to equation 3.9.
- Determine the life of each critical position. Refer to equation 3.10.

When calculating the number of cycles to failure, each critical position must individually be assessed. The fracture stress (σ_f) is determined using an appropriate fatigue code [9], [15], [40]. Each critical position must be put equivalent to the appropriate weld category. Refer to section 2.4.3, page 31.

$$N_c = \left(\frac{\Delta \sigma_c}{\sigma_f} \right)^{\frac{1}{b}} \tag{3.8}$$

$$D_c = \frac{n_{eqv}}{N_c} \tag{3.9}$$

$$L_c = \frac{1}{D_c} \tag{3.10}$$

3.2 Closure

This chapter formalized the methodology of solving a structural fatigue related problem, using the Fatigue Equivalent Static Load method. Various case-studies are presented to show the usage of this methodology. The following chapter will present these case-studies to the reader.

Chapter 4

CASE-STUDY DEFINITION

4.1 Scope

This chapter discusses the various case-studies that were done to illustrate the theories of the Fatigue Equivalent Static Load method. The four case-studies are as follows:

- Aluminum dry-bulk tanker
- Sub-frame of a pick-up truck
- Suspension bracket of a large passenger bus
- Suspension bracket of a 4x4 pick-up truck

4.2 Aluminum Dry-bulk tanker

Various transport vehicle manufacturers have, due to the competitive nature of the transport industry, started manufacturing vehicles with lighter materials for example aluminum. This vehicle was instrumented and measured during a routine trip that would give a good indication of the loads the vehicle would experience (refer to figure 4.1). A finite element model of the $40m^3$ dry-bulk

Figure 4.1: Aluminium dry bulk tanker

tanker was created . The finite element model was subjected to a fatigue equivalent static load that was determined using measurements obtained during the measurement exercise (refer to figure 4.1).

4.3 Sub-frame of a pick-up truck

The need has arisen in the industry to supply a vehicle with a detachable load bay. The load bay (or swap-body) is an enclosed structure specifically designed to meet the requirements of the client. The sub-frame assembly would act as an interface between the chassis and the swap-body. The concern was raised that the chassis, on which the swap-body will fit, may endure a concentrated bending and twisting deformation in the area between the cab and the front most swap-body mounting. This is due to the fact that the swap-body is substantially stiffer than a normal load box. This problem could have dire consequence for the vehicle manufacturer. Rubber mounts between the chassis and the sub-frame would reduce this problem.

A quasi-static load was initially used to design a prototype sub-frame. Several iterations were done to optimize the design. The prototype sub-frame was used in the mock-up configuration during the first measurement exercise to obtain load inputs to the vehicle structure. The measurements obtained

Figure 4.2: Pick-up truck , with sub-frame and swop body

from the vehicle were used to calculate the loads of the dynamic analysis. The purpose of the dynamic analysis was to obtain the optimum rubber stiffness that is needed to isolate the swap-body from the chassis. The stiffness of the rubber should, however, not cause the swap-body to resonate. This was also addressed with the dynamic analysis. Recommendations were subsequently made regarding the rubber stiffness. The final part of the exercise was to verify the fatigue life expectancy of the pick-up truck's chassis. This was done by taking similar analysis measurements of a fully configured vehicle. The measurements were processed and fatigue calculations carried out. The result of these calculations was another quasi-static load that is applied to the chassis and the sub-frame. The results of these analyses are then evaluated using the European structural fatigue code [15].

4.4 Suspension bracket of a large passenger bus

This case-study deals with the design verification of the suspension bracket implemented on the tag axle of a large passenger bus. The suspension bracket previously used by the manufacturer experienced failures after a relatively short life in the field. The finite element analysis was used to determine displacements and stress levels based on given static forces determined by force and strain measurements. The static load on the FE model is calculated as follows:

- The force versus time data is subjected to a 'rain-flow' [1] [15] counting method. The result of this analysis will be used to calculate the respective damages to each measurement file.
- The accumulated damages for the test period can be computed, using Miner's law of linear damage accumulation [1]. The accumulated damage is used to compute a force (repeated 2×10^6 times) that is equivalent to the dynamic input to the structure.
- The equivalent static force is applied to the finite element model. The stresses are then evaluated according to the ECCS code for the fatigue design of steel structures [15]. The finite element analysis' stress results will be compared to the fatigue strength curves in the ECCS code to determine the fatigue life.

4.5 Suspension bracket of a 4x4 pick-up truck

This case-study investigated a shock absorber bracket that experienced failures on the vehicle manufacturer's durability track. The purpose of the case-study was to determine the cause of the cracking failure of the bracket after 35 000 km on the durability track and to propose a modified design. The project consisted

Figure 4.3: 4x4 pick-up truck

of an instrumentation and measurement phase, a data analysis phase, a finite element analysis phase and a fatigue assessment phase (refer to figure 4.3).

4.6 Closure

All of the case-studies were subjected to the same methodology formulated in the previous chapter. The following chapter will deal with the first phase of the Fatigue Equivalent Static Load method, namely the measurement phase.

Chapter 5

DETERMINATION OF INPUT LOADING

5.1 Scope

This chapter deals with the measurements of the various case-studies. The measurement of the loads that a vehicle will experience is an integral part of the design/assessment procedure. It is essential to determine the loads that the respective structures would have to endure throughout the course of their life-times. The measurement of loads is often neglected due to the uniqueness and the difficulty in obtaining the loads, especially during the design or assessment of fatigue loaded vehicle structures.

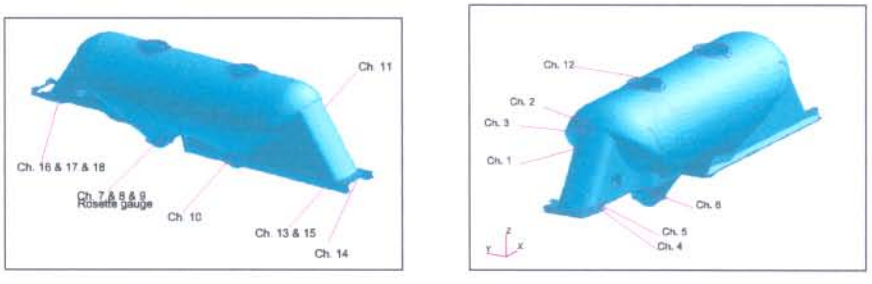

Figure 5.1: Bulk tanker: measurement positions

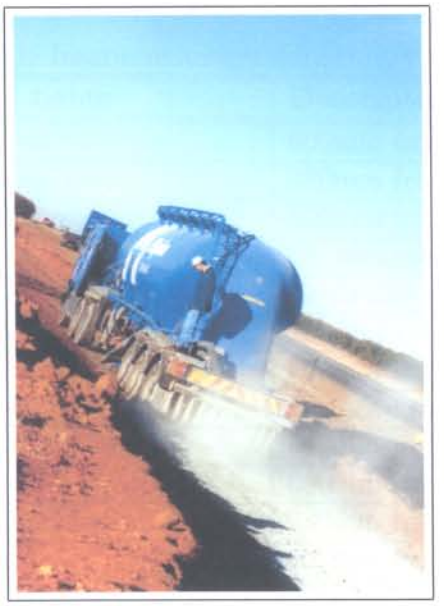

Figure 5.2: Bulk tanker: spreading operation, Heidelberg, Gauteng

5.2 Aluminum Dry-bulk Tanker

The aim of this measurement exercise was to determine the stresses/strains that the vehicle structure experiences during its life-time. These measurements, in conjunction with a finite element model, can then be used to determine a fatigue equivalent static load. This load can further assist in the optimal design of the vehicle structure.

5.2.1 Instrumentation

The tanker was instrumented using eighteen channels. Twelve of the channels were dedicated to strain gauge measurements and the remaining six channels used to measure the six degrees of freedom with the use of accelerometers (refer to table 5.1). Also refer to figure 5.1. The channels were digitally recorded with three *Spiders*[1] on a portable laptop computer.

[1]Spiders are electronic equipment specifically designed for multi-channel measurements

Table 5.1: Instrumentation detail - dry bulk tanker

Chan	Channel name	Description/position
1	Front boom	600mm from top of boom (vertical)
2	Front boom weld	300mm from centre, near top weld
3	Front dish weld	500mm from centre, dish to shell weld
4	Compressor mount	On compressor beam (on top-flange)
5	5th Wheel box member	Centre of pocket of rear cross-member
6	Side-plate bend front	10mm from both weld edges (vertical)
7	Rosette vertical	600mm from centreline of cone
8	Rosette 45 degrees	as above mentioned
9	Rosette horizontal	as above mentioned
10	Outer cone rear	630mm from centreline (vertical)
11	Rear boom centre	830mm from bottom of chassis
12	Top shell front	400mm from centre of top shell

5.2.2 Measurement trip

The opportunity arose to measure strains during a trip from Brakpan to a mine near Tzaneen. The trip encompassed various road conditions. The measurements started at Alpha Cement's depot at Brakpan, followed by secondary roads and highways enroute Pretoria. The N3 highway from Pretoria to Pietersburg was a relatively smooth stretch. From Pietersburg to Tzaneen, the tanker experienced various degrees of road surfaces. The Duiwelskloof pass with its steep decent, potholes and road improvement surface, proved to be a worthwhile candidate for the measurement exercise. A typical secondary road was measured from Tzaneen to the turn-off at the Marinda mine. The road to the Marinda mine was found to be an especially rough gravel road. Additional maneuvering at the mining complex was also measured.

Two days after the first measuring exercise, the tanker's performance was measured during a spreading operation. The measurements again started at Alpha Cement's depot in Brakpan. Secondary and highway surfaces were measured on the way to a building site near Heidelberg. Measurements encompassed a gravel road, maneuvering at the site, as well as the spreading operation (refer to figure 5.2).

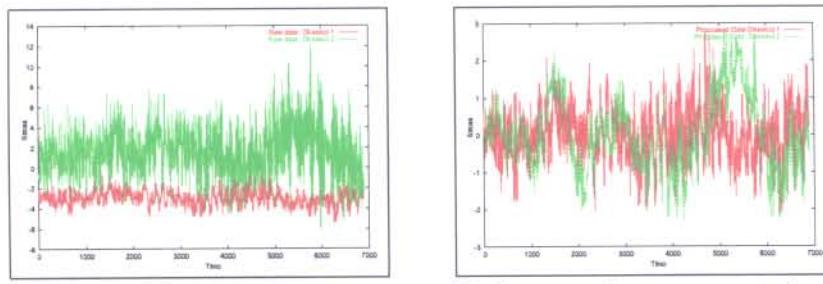

(a) Raw measurement data (b) Proccessed measurement data

Figure 5.3: Measurement data

5.2.3 Measurement Data

During the two measurement exercises, a total of 114 usable files were recorded. The sampling frequency of the measurements was 300Hz. A few files exhibited spikes (extremely large peaks of stresses). These large peak stresses occurred randomly in some of the measurement files. The spikes also occurred randomly at the different channels. If a large force is applied to the structure, the strain gauges in the vicinity will experience deformations. The random occurence of very high stresses at different strain gauges, at different time intervals, indicated that these data is not because of input loads, but of measurement equipment defects. The integrity of all the files was assured with a *Matlab* program that removed all these spikes. The files also exhibited some drift over a period of time (a common occurence while measurements are taken over a long period of time, [4]). These drift tendencies were also removed with a *Matlab* program. Refer to figure 5.3(b) and 5.3(a) to view the raw and processed data.

5.2.4 Summary

The measurement exercises supplied the data to be processed in conjunction with the finite element model. The data will then be used to calculate a fatigue equivalent static load, as described in Chapter 6.

5.3 Sub-frame of a pick-up truck

The pick-up truck measurement was done in two phases. The initial measurements were taken on a vehicle with a prototype swap-body assembly. These measurements were mainly used for a dynamic analysis. The second measurement exercise, using the correct configuration, was used to calculate the fatigue damage.

5.3.1 Phase 1 measurements: prototype vehicle

The vehicle with the mock-up configuration was instrumented with strain gauges, a displacement transducer and accelerometers to obtain the input loading from the road surface. Figure 5.4 indicates a typical measurement position. The following sections were measured at Gerotek:

- Suspension track, driven at a speed of $10km/h$.
- Suspension track, driven at a speed of $20km/h$.
- Sinus, in-phase track.
- Sinus, out-of-phase track.
- Circular track, clockwise at $30km/h$.
- Gravel track.

The measurements were taken at a $400Hz$ frequency.

5.3.2 Phase 2 measurements: final vehicle

Measurements were taken on a vehicle with the correct configuration. The aim of the measurement exercise was to determine a fatigue equivalent static load that can be applied on the static finite element model. These measurements can also be used to calculate the fatigue life of the area where the half bridge strain gauges were applied. Two measurement exercises were performed on

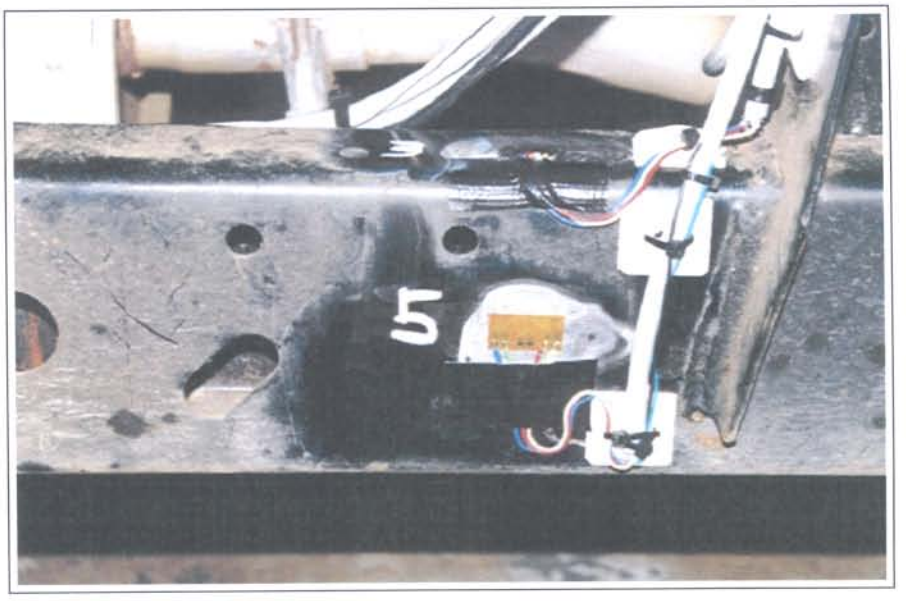

Figure 5.4: Strain gauge measurement equipment

the new vehicle. The first measurement was done on a vehicle with temporary rubbers at the sub-frame connection. The correct swap-body and sub-frame was, however, installed on the vehicle. The second measurement exercise was performed on a vehicle with the correct rubber mounts, as well as a new leaf-spring configuration. The *first* measurement exercise included the following surface sections:

- Gravel
- Secondary tar
- Highway

The *second* measurement exercise consisted of a fully loaded vehicle travelling only on gravel and secondary tar. These measurements can be combined to create a user profile of what the vehicle would endure during its lifetime. Figure 5.5 displays the strain gauge measurements taken on the gravel track.

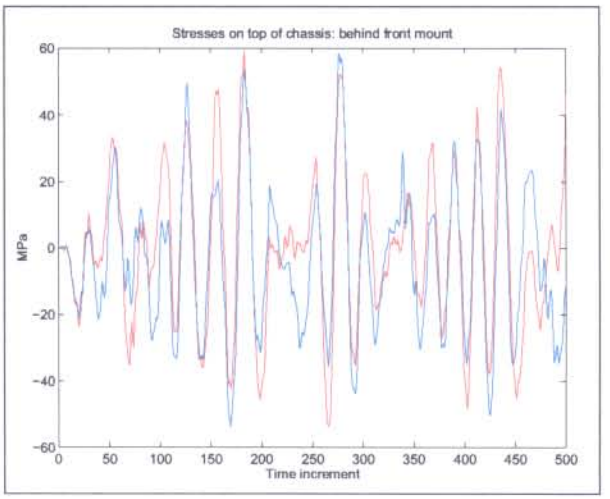

Figure 5.5: Strain gauge measurements - sub-frame

5.3.3 Summary

The measurement exercises provided the data needed for the calculation of the fatigue load to which the vehicle would be subjected. The following chapter will indicate how the measurement data were processed into useful fatigue information.

5.4 Suspension bracket of a large passenger bus

Measurements were performed on the bus in question. The tag axle was instrumented on both sides. Due to the shock absorber manufacturer's reluctance to provide the shock absorber characteristics, the left-hand shock absorber was instrumented on the shaft. This was necessary to measure the force exerted by the shock absorber on the suspension bracket. Measurements were taken on three different road surfaces: highway, secondary tar and gravel. The measurements were also conducted with a fully laden vehicle as well as an empty vehicle. The results of these different measurements were later used in the

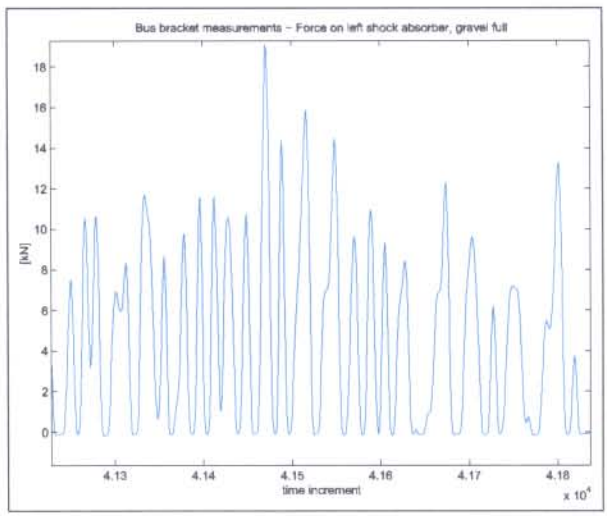

Figure 5.6: Measurement data - Bus bracket

fatigue analysis to create a combined road usage profile. Refer to figure 5.6.

5.5 Suspension bracket of a 4x4 pick-up truck

The client required that the component must be able to withstand a predetermined life-time on a durability track. The input forces of the shock absorber, as well as strains at two locations on the component, were measured.

Table 5.2: Measurement Channels - 4x4 pick-up suspension bracket

Chan.	Description/position	Purpose of measurement
1	Left wheel front shock absorber bracket strain gauge	Reference for FEA, at assumed crack initiation position
2	Left wheel front shock absorber bracket strain gauge	Reference for FEA
3	Left wheel front shock absorber displacement metre	Vertical relative velocity of shock absorber to calculate force on bracket

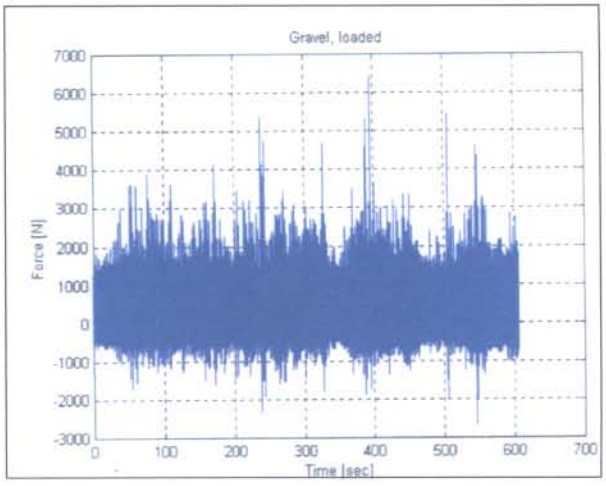

Figure 5.7: Input load measurements - 4x4 pick-up

5.5.1 Measurements

Table 5.2 lists the measurement channels that were applied. Figure 7.7 also shows the position of the cracking experienced during the durability testing. The measurements were successfully completed on representative sections of a durability route. This included empty and loaded measurements on the logs and track sections, as well as sections of the tarred and gravel roads on the route.

5.5.2 Calibration and Data Processing

The sampling frequency was $150Hz$. The measured displacement was calibrated ($1Volt = 180mm$) and then digitally differentiated to obtain velocity versus time data. This data was converted to force versus time data, using the characteristics of the shock absorber listed in Table 5.3. The force results for the loaded condition on the logs, track, gravel and tarred sections are depicted in Figure 5.7

The strain gauge data was converted to stresses, assuming linear elastic behaviour. The stresses were found to be small, implying that the crack does

Table 5.3: Shock absorber characteristics - 4x4 pick-up truck

Extension or Compression [m/s]	Tensile Force [N]	Compressive Force [N]
0.1	1330	410
0.3	1990	725
0.6	3040	1150
1.0	4550	1800

not initiate on the edge of the bracket. The measured force versus time histories were subsequently calibrated using the finite element model (refer to equation (5.1)) The measured data now consists of stress versus time data.

$$S_{cal} = \left(\frac{S_{FEA}}{F_{FEA}}\right)_{cal} \times F_{meas} \tag{5.1}$$

where :

S_{cal} = calibrated stresses

S_{FEA} = calculated FEA stress

F_{FEA} = applied FEA force

F_{meas} = measured forces

5.5.3 Summary

The input loading of the shock absorber was determined for various loading conditions experienced on the durability route. The input load data was converted to measured stress data, using finite element calibration, and can now be used in the fatigue processing as described in the next chapter.

5.6 Closure

This chapter dealt with the measurement process of obtaining the fatigue loads to which the vehicle structures were subjected to. The various case studies illustrate a few different methods of obtaining these loads. The following chapter will discuss the fatigue calculations performed for the case-studies.

Chapter 6

FATIGUE CALCULATIONS

6.1 Scope

The previous chapter showed through various case-studies how the fatigue loads of the vehicle structures were measured. This chapter will show, using the different case-studies, the methodology in converting the measured data into a fatigue equivalent static load.

6.2 Aluminum Dry-bulk Tanker

The following methodology was used to calculate the fatigue equivalent stress that the $40m^3$ aluminium Spitzer tanker experienced during the measurement exercise. All the strain gauge measurement channels were used to calculate the damage experienced during the two trips. The spreading exercise was analysed separately from the Tzaneen excursion. The two separate damages will be used to calculate an accurate damage that a typical vehicle will experience throughout its life. The damages of all the data files were calculated as follows: the data generated by the pre-processing, is analysed with the use of the so-called *rain-flow* algorithm. The end result of this exercise is a table in which different stress amplitudes are displayed, with its various occurrences (refer to table 6.1). This table gives the following information: The table shows that

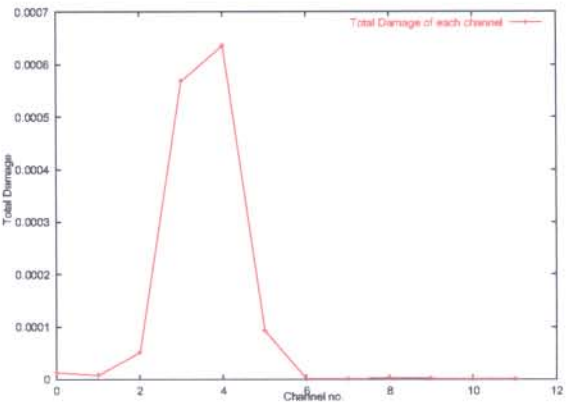

Figure 6.1: Damage measured during Tzaneen trip

a certain stress ($\Delta\sigma_i$) was repeated n_i times during the test trip. For example, the vehicle was subjected to an amplitude stress of 0.034 MPa that was repeated 268 times. The following step in the whole procedure is to evaluate the results of the rain-flow counting exercise. The stress-life equation [1] is used to calculate the amount of cycles (N_i) for each stress range ($\Delta\sigma_i$). Refer to equation (2.6), page 21.

The σ_f value, is selected arbitrary from the aluminium structural code [9] (as long as the value is bigger than the $\Delta\sigma_i$ value). The b value is selected using the assumption that the fatigue fracture will occur at a weld. The value of b is $-1/3$. The N_i and n_i values are now used in Miner's damage equation (2.12), page 29. Figure 6.1 displays the total damage of each channel for the measurement trip to Tzaneen. (This damage *does not* include the spreading operations data) The above-mentioned procedure was carried out with the help of custom programmed *Matlab* programs.

The assumption is made that while the vehicle travelled from Brakpan to Tzaneen, an average speed of 80 km/h was maintained. The total distance of measured data recorded is thus 110 km. The damage (D_{110km}) is subsequently calibrated of measurements during the Tzaneen trip. The data of the spreading exercise must, however, also be considered. The same procedure is

Table 6.1: Rain-flow results - dry bulk tanker

$\Delta\sigma_i$ [MPa]	n_i (cycles)
0.0168	42
0.0337	**268**
0.0506	181
0.0675	124
0.0844	102
0.1013	78
0.2365	10
0.3379	3
0.3886	1
0.4731	1

followed for the spreader measurement exercise to calculate its damage (D_{sprd}). The assumption is made that 5% of the vehicle's life is dedicated to similar spreading exercises. It is also assumed that the vehicle travels at an average speed of $10\,km/h$. The vehicle thus travels the equivalent of $23km$ during the measurement period.

The total damage (D_{tot}) can thus be calculated if it is assumed that the vehicle would travel $1\,000\,000\,km$ during its lifetime. Refer to equation 6.1.

$$D_{tzan} = \left(\frac{1\,000\,000km - 50\,000km}{110\,km}\right) \times D_{110km}$$

$$D_{sprd} = \left(\frac{50\,000km}{23\,km}\right) \times D_{23km}$$

$$D_{tot} = D_{tzan} + D_{sprd} \tag{6.1}$$

With the *total* damage known (D_{tot}), the equivalent stress range can now be calculated, using equation (6.2). Refer to table 6.3 to view the results.

Table 6.2: Total damage - dry bulk tanker

Channel no	D_{tzan}	D_{sprd}	D_{tot}
1	0.11347	0.00123	0.11470
2	0.07204	0.00195	0.07399
3	0.44689	0.01253	0.45943
4	4.90476	2.33337	7.23813
5	5.49477	0.33796	5.83273
6	0.81144	0.09027	0.90171
7	0.01332	0.00100	0.01432
8	0.00711	0.00057	0.00768
9	0.03029	0.00216	0.03245
10	0.02401	0.00193	0.02594
11	0.01050	0.00055	0.01105
12	0.01313	0.00079	0.01393

The σ_f value is arbitrarily chosen from the ECCS code [15], bearing in mind this value is cancelled out after further substitution in the fatigue equivalent equation. The σ_f value must be 'chosen' so that it is bigger than the $\Delta\sigma_i$ value.

$$\Delta\sigma_{eqv} = \left(\frac{n_{eqv}}{D_{tot}}\right)^b \sigma_f \tag{6.2}$$

where :

σ_{eqv} = equivalent stress

n_{eqv} = equivalent number of cycles (usually two million)

σ_f = fracture stress

D_{tot} = total damage

b = Basquin's fatigue strenght exponent

The finite element model was then subjected to a *unit vertical gravitational acceleration* load. The resultant stresses (S_{FEA}) of the finite element analysis are used to calibrate the results of the measurement exercise. Re-

Table 6.3: Equivalent stress results - dry bulk tanker

Channel no.	$\Delta\sigma_{eqv}$ $[MPa]$ (Tzaneen)	$\Delta\sigma_{eqv}$ $[MPa]$ (Spreading)	$\Delta\sigma_{eqv}$ $[MPa]$ (Combined)	S_{FEA} $[MPa]$ (Combined)	a_{eqv} $[g]$
1	11.62	2.57	11.66	24.8	0.47
2	9.98	3.00	10.07	28.0	0.36
3	18.35	5.57	18.51	23.5	0.79
4	42.35	16.71	43.20	18.2	2.55
6	22.38	10.76	23.18	18.8	1.23
10	6.92	2.98	7.10	14.3	0.50
11	5.25	1.96	5.34	6.03	0.89
12	5.66	2.22	5.77	12.1	0.48

fer to figures 6.2(a) and 6.2(b) to view the finite element calibration stresses. The equivalent acceleration load is calculated using equation 6.3. It should be noted that the stress comparison is done on the *same* geometric position on the vehicle. Not all the strain gauge channels were used to calculate the equivalent acceleration load. The rosette gauge (channels 7-9) and the strain gauge in the pocket of rear-boom cross-member (channel 5) are omitted in the calculations. The rosette gauge's data is used to calculate the principal stresses (verification purposes), while channel 5 measures the *shear* stress concentration in the rear cross-member pocket. The equivalent acceleration (a_{eqv}) represents a fatigue load that the vehicle would endure over 1 million kilometers. The equivalent acceleration load can now be used to evaluate the structure.

$$a_{eqv} = a_{cal} * \frac{\sigma_{eqv}}{S_{FEA}} \tag{6.3}$$

where :

a_{eqv} = equivalent acceleration load

a_{cal} = calibration acceleration load applied in the FEA to obtain S_{FEA}

σ_{eqv} = equivalent stress

S_{FEA} = Calibration or calculated stress using a FEA

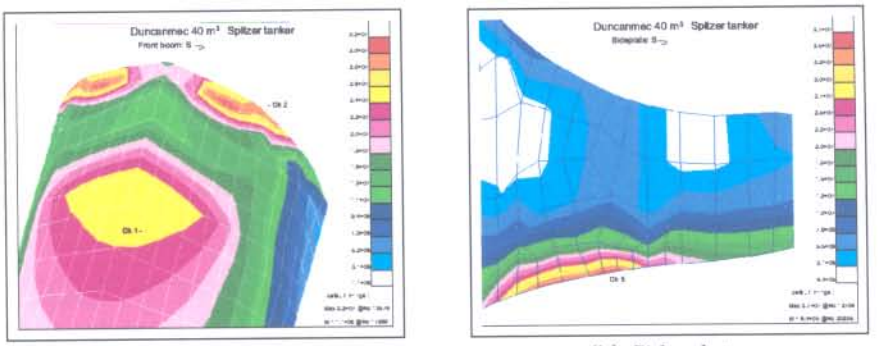

(a) Front boom (b) Side plate

Figure 6.2: Bulk tanker - calibration stresses

The fatigue calculations of the data measurement exercises showed the following: A maximum load of $2.551g$ was calculated with the measurement data. This load was calculated at *channel 4*, on the outrigger of the compressor mounting (refer to table 6.3). The outrigger can be viewed as a cantilever beam with a large point load. The dynamic behaviour of the beam can therefore deform in higher order bending deformations. The Fatigue Equivalent Static Load method makes use of a calibration stress (using a FEA) in a first order bending mode. The FESL load calculated using these strain gauge measurements is therefore not accurate, and may be omitted. The following high quasi-static load occurred at *channel 6*, on the side plate. A load of $1.233g$ was calculated at the measurement point. This calculated load is near a *stress concentration*, and can therefore not be accurately interpreted. The rest of the channels gave results ranging between $0.36g$ and $0.89g$. The average of all the quasi-static loads is approximately $0.58g$.

The outcome of the fatigue calculations performed on the measurements gave excellent results regarding the usage of the FESL method. Channel 4 showed, as predicted, that higher order dynamic behaviour can not be used with the Fatigue Equivalent Static Load method. Channel 6 indicated the dangers of extrapolating measurements near high stress concentrations. The

Table 6.4: Final calibrated measurements - sub-frame of pick-up truck

Measurement position	Description	Damage (per file)	% of tot. life	Damage	a_{eqv} $[g]$
Right side bot. (channel 10)	Gravel, full	0.1111E-4	0.5	1.11	
	Secondary, full	0.1193E-4	0.5	0.99	
			Total DAMAGE	1.0531	**3.1**
Left wheel (channel 8)	Gravel, full	0.1037E-4	0.5	1.04	
	Secondary, full	0.0828E-4	0.5	0.69	
			Total DAMAGE	0.8642	**2.1**
Right wheel (channel 9)	Gravel, full	0.1393E-4	0.5	1.39	
	Secondary, full	0.0686E-4	0.5	0.57	
			Total DAMAGE	0.9825	**2.6**

rest of the channels showed an excellent correlation, with a narrow band of acceleration results. The narrow band of loads gives the designer confidence to extrapolate these loads to the whole structure.

6.3 Sub-frame of a pick-up truck

A profile of road usage was created so that the amount of damage can be calculated. The profile ratio is: 10:35:55 (gravel, secondary tar, highway). The high percentage chosen for highway usage includes usage on good secondary roads. The assumption was made that the total life-time of the vehicle will be 200 000 km. The second measurement exercise consisted only of gravel and secondary tar, while the vehicle was fully loaded. A ratio was therefore calculated to take the highway and empty damage into account (using the data obtained from the first exercise). The calculations showed a ratio of approximately two between the damage accumulated during gravel and secondary tar measurements, and the highway measurements. The *second* measurement exercise was also subjected to a fatigue calculation where the damage was calculated. The data of the two measurement exercises was processed and combined to give an accurate and realistic total damage figure (refer to table 6.4).

The total damage was used to calculate a fatigue equivalent vertical ac-

Table 6.5: Rain-flow results on left bracket - bus bracket

Amplitude Forces Δf_i $[N]$	**Mean Forces** $[N]$	**Reversals** n_i (cycles)
471	26304	70
941	25833	428
3295	23480	448
3765	23010	320
4236	22539	262
4706	22068	**130**
8001	18774	23
8472	18303	13
9884	16891	12
10354	16420	8
10825	15950	4
12708	14067	2
13178	13597	1
13649	13126	1

celeration cycle range (Δa_{eqv}), using equation 6.2, page 69. The equivalent load would cause the same damage as the modified measurements (if repeated 2×10^6 times). This vertical acceleration would therefore occur 2 million times during the 200 000 km (refer to table 6.4). An average vertical acceleration of $2.5g$ was applied on an FE model. The fatigue analysis was done using the stress results of the FE analysis. The chassis was evaluated using the European structural fatigue code [15], where the stresses calculated are treated as stress ranges, repeated 2×10^6 times during the life.

6.4 Suspension bracket of a large passenger bus

The following analysis was done to calculate the actual damage that the suspension bracket experienced during the measurement exercises.

Table 6.6: Damage Calculations on left bracket - bus bracket

File name	Load Condition	Distance $N_{meas}\,km$	Road Surface	D_{file}
ctctle.mat	Empty	$5.5\,km$	Secondary Tar	397.6
ctctpful.mat	Laden	$5.5\,km$	Secondary Tar	407.9
ctchwful.mat	Laden	$6.5\,km$	Highway	152.4
ctcgrful.mat	Laden	$3\,km$	Gravel	555.0

6.4.1 Equivalent static force

The damage of the data files of the measured shock absorber forces are calculated as follows: the data is analysed with the use of the *rain-flow* algorithm [15]. The end result of this exercise is condensed in a table in which different force amplitudes, mean forces and their corresponding reversals are shown (refer to table 6.5). Table 6.5 gives the following information: the table shows that a certain force (Δf_i) was repeated n_i times during the test trip. For example, the bracket was subjected to an amplitude force of $4706N$ that was repeated 130 times.

The following step in the whole procedure is to evaluate the results of the rain-flow counting exercise. The stress-life equation [1] is used to calculate the amount of cycles (N_i) for each force range (Δf_i) (refer to equation (2.6), page 21). It should be noted that ECCS code contains stress data. The stress data is calibrated to a force by means of the finite element model. The b value is selected based on the assumption that the fatigue fracture will occur at a weld. The value of b is $-1/3$. The N_i and n_i values are now used to calculate the damage in Miner's damage equation (2.12). The above-mentioned procedure was carried out with the help of the *Matlab* programs.

The damages calculated by equation (2.12) are calibrated to constitute a damage equal to a lifetime of 3 000 000 km. Refer to equation (6.4).

$$D_{file} = \left(\frac{3\,000\,000 km}{S_{meas}\,km}\right) D_{per\,file} \tag{6.4}$$

where :

D_{file} = calibrated damage of the measurement file
S_{meas} = distance of the measurement file
$D_{perfile}$ = actual damage of the measurement file

These damages are calculated for each measurement file. The damages (D_{file}) are then combined according to the user profile, as supplied by the client. The following equations show two user profiles. Refer to equations (6.5) and (6.6). Also refer to table 6.6 and table 6.7.

$$\begin{aligned} X &= (D_{ctctle} + D_{ctctpful})/11\,km \\ Y &= D_{ctchwful}/6.5\,km \\ Z &= D_{ctcgrful}/3\,km \end{aligned}$$

$$D_{up1} = (X \cdot 40\% + Y \cdot 50\% + Z \cdot 10\%) \times 3\,000\,000 km \tag{6.5}$$

$$D_{up2} = \left(\frac{D_{ctctle} + D_{ctctpful}}{11\,km}\right) \times 3\,000\,000 km \tag{6.6}$$

where :

D_{up1} = damage of user profile one
D_{up2} = damage of user profile two

The following step is to calculate the *fatigue equivalent stress range* ($\Delta\sigma_{eqv}$) for 2×10^6 cycles, that will equal the combined damages. This is done using equation (6.2), page 69. The finite element model is subsequently employed to calibrate the FEM *force* relative to the fatigue equivalent static stress ($\Delta\sigma_{eqv}$). Table 6.7 displays the equivalent forces for the combined damages for the left

Table 6.7: Equivalent Forces - bus bracket

User Profile No.	Left		Right	
	Damage (D_{up*})	ΔF_{eqv} $[kN]$	Damage (D_{up*})	ΔF_{eqv} $[kN]$
1	178.55	56.21	0.82	9.36
2	219.69	60.23	1.55	11.6

and right bracket (D_{up1} & D_{up2}).

6.4.2 Data and analysis verification

During the measurement exercise, only the left suspension bracket input forces were measured. To ensure the integrity of the measurement exercise, especially regarding the right suspension bracket, the above mentioned exercise was verified. The verification was done using the following methodology:

- The finite element stresses at the strain gauge position are obtained from the FE model.
- The strains that cause these stresses are calculated through solving equations 6.7, 6.8 and 6.9 simultaneously.
- A relationship between a force and the strain at the measurement position is therefore established ($C_{cal} = F_{fem}/\epsilon_{fem}$).
- The following step is to compare the measured strains to the measured forces, using the multiplication factor (C_{cal}). The measured strains and forces clearly corresponded with each other.

$$\sigma_x = E\left(\epsilon_x - \nu(\epsilon_y - \epsilon_z)\right) \tag{6.7}$$

$$\sigma_y = E\left(\epsilon_y - \nu(\epsilon_x - \epsilon_z)\right) \tag{6.8}$$

$$\sigma_z = E\left(\epsilon_z - \nu(\epsilon_x - \epsilon_y)\right) \tag{6.9}$$

It is thus shown that the *calculated* finite element stress at the position of the strain gauge compares very favourably with the *measured* stresses. The resulting stresses on the FE model can therefore be linearly calibrated to the required fatigue equivalent stress range ($\Delta\sigma_{eqv}$). The fatigue equivalent static force for the right suspension bracket can subsequently also be calculated ($\Delta F_{eqv} = X_{FEA}\Delta\sigma_{eqv}$). Refer to table 6.7.

6.5 Suspension bracket of a 4x4 pick-up truck

6.5.1 Fatigue life prediction on existing design

In Chapter 5 it was shown how the measured force histories were converted to stress histories (refer to equation (5.1), p.64). Material fatigue properties were assumed, based on the tensile properties of the material. The damages calculated for each of the measured sections were appropriately accumulated to obtain the correct mix of tar, gravel, track and log sections for one cycle of the durability route (D_{cycle}). The distance to failure (s_{fail}) was subsequently calculated using equation (6.10). The original component failed at 35 000 km ($s_{fail} = 35\,000\,km$). The measurement data, as well as the FE model could therefore be calibrated to give a realistic representation of the component.

$$s_{fail} = \frac{1}{D_{cycle}} \times s_{cycle} \tag{6.10}$$

where :

s_{fail} = distance to failure

D_{cycle} = damage of one cycle

s_{cycle} = distance of one cycle of the durability route

Figure 6.3: Original suspension bracket - 4x4 pick-up truck

6.5.2 Fatigue criterion for modified design

The modified component must at least survive 120 000 km on the durability route ($s_{fail} = 120\,000\,km$). Based on the same calculations performed for the existing design, a fatigue criterion for a modified design was derived. Assuming that the component is modified with additional welded components, using the fatigue properties prescribed by BS 7608: 1993, the calculations indicated that the nominal stresses adjacent to the weld should, for a specific calibration input load, not exceed 4 MPa. For the parent metal, peak stresses away from welds should be below 10 MPa for the applied loading.

6.5.3 Qualification testing

Durability rig testing was performed on a *baseline* (original design) bracket (see figure 6.3), as well as a prototype modified bracket (see figure 6.4). The testing was performed using a servo-hydraulic actuator, inducing single amplitude sine

Figure 6.4: Modified suspension bracket - 4x4 pick-up truck

wave loading onto the bracket. The amplitude of loading was fixed to be equivalent to the average measured peak-to-peak loading experienced on the logs section. Based on fatigue calculations, it was estimated that it would be required to complete 1.6 million cycles of the rig testing to induce the same damage as would 120 000 km of durability route testing.

During the actual testing, the baseline specimen survived for 126 400 $cycles$ before failing. The modified design was only tested to 800 000 $cycles$ (without failing), implying a maximum life expectancy of 222 000 km in terms of a durability route distance.

6.6 Closure

The chapter illustrated how measurement data is processed into fatigue equivalent static loads. The case-studies indicated the various methods of calculating the damages that were measured. These damages were then used to calculated the FESL loads, that can be used to assess a vehicle structure. The chapter

also showed the use of the finite element process to obtain these fatigue loads. The following chapter will describe how the FE models were created and used in solving the fatigue loads, and deal with various structural problems.

Chapter 7

FINITE ELEMENT STRUCTURAL ANALYSIS

7.1 Scope

The finite element analysis is an essential and valuable tool to assess the integrity of a structure. As mentioned in the previous chapters, the finite element analysis can be used during the various phases of the fatigue equivalent static load method. Chapter 5 illustrated how the data was measured. In Chapter 6 the resulting damages were used in conjunction with the FE calibration stresses to calculate the fatigue equivalent static load. This chapter deals with the finite element analyses of the various case studies.

7.2 Aluminum Dry-bulk Tanker

Geometry and Finite Element Modelling

The geometry of the finite element model was created using the manufacturer's drawings of the vehicle. These drawings included the shell assembly, item lists and assembly drawings of the front and rear assemblies. Unigraphics (UG), an advanced 3-D CAD program, was used to create all of the trailer parts. UG

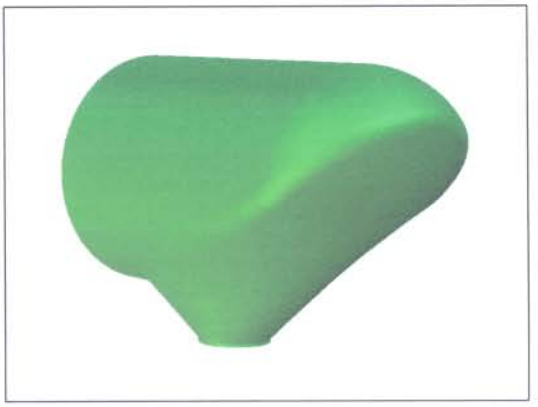

Figure 7.1: Unigraphics CAD model - hull

was especially useful to create the complex geometry of the tank shells (refer to figure 7.1). The 3-D geometric model was then imported into a finite element modeller, *MSC.Patran*. In the *Patran* package, the complex geometry was processed to create the finite elements that form the core of the analysis. Shell elements were used to create the Spitzer Tanker (refer to figure 7.2). The whole model, with all its different components, was analysed with a finite element analysis solver called PERMAS. After the model was analysed by PERMAS, the results were viewed in *Patran* for further evaluation.

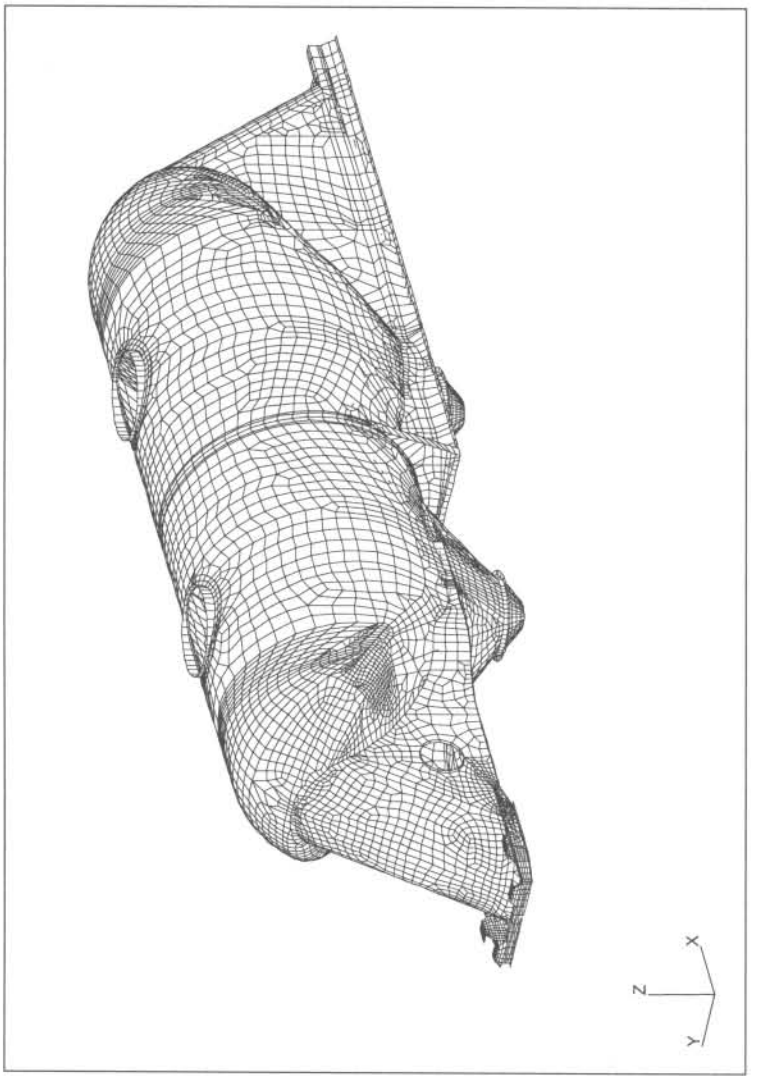

Figure 7.2: Bulk tanker - Finite Element Model

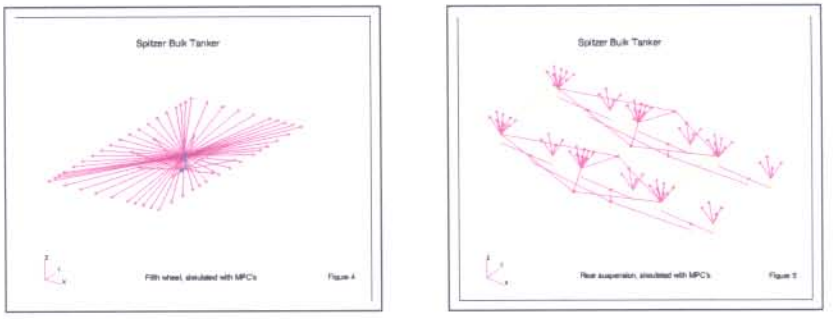

(a) Kingpin MPC, bulk tanker (b) Rear suspension

Figure 7.3: Multiple Point Constraints - bulk tanker

Materials and element properties

The material properties of the Spitzer tanker was aluminum. A Young's modulus of 80 GPa and the Poisson ratio of 0.3 was used. The properties were assigned to the mid-plane of the elements.

Loads and Boundary conditions

The model must however also be constrained. This is done at the fifth wheel and the suspension of the tanker. The fifth wheel, as well as the suspension is simulated with the use of MPC's[1] (refer to figure 7.3). The following equation was used to calculate the fatigue load case. The fatigue equation was based on the inputs obtained from the fatigue calculations stipulated in Chapter 5.

$$LC_{fat} = 0.58a_{vert} + 0.58P_{vert}$$

where :

a_{vert} = unit load, vertical acceleration

P_{vert} = unit load, vertical pressure

[1]Multiple Point Constraints

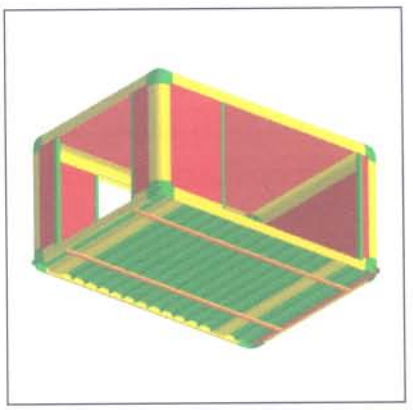

(a) Unigraphics CAD model - swop body

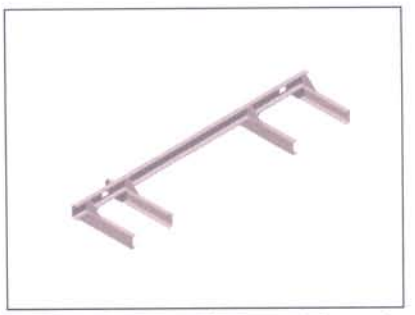

(b) Unigraphics CAD model - sub-frame

Figure 7.4: Unigraphics CAD models - sub-frame of pick-up truck

7.3 Sub-frame of a pick-up truck

Geometry and Finite Element Modelling

- *Chassis:* The chassis geometry was created using IGES and TIFF files that were supplied by the client. The chassis was subsequently modelled using a CAD package (Unigraphics) and exported to *MSC.Patran* for the finite element modelling.

- *Swap-body:* The geometry of the swap body was created in Unigraphics, using drawings supplied by the manufacturer (refer to figure 7.4). The finite element modelling was performed using *MSC.Patran*.

- *Cab:* Geometry of the cab was created in *MSC.Patran*. The geometry was created bearing in mind that the cab mounts to the chassis. The cab is only representative of the real article, and was created with the intention to achieve the correct stiffness of the whole structure.

- *Sub-frame:* The sub-frame was designed in Unigraphics (refer to figure 7.4). Special care needed to be taken to ensure that the sub-frame had the correct interface parameters with respect to the swap-body and

the vehicle chassis. The manufacturing aspects also played an important part in the design of the sub-frame. The geometry of the model was generated using the advanced parametric capabilities of Unigraphics. This was necessary if iterations were to be done on the sub-frame.

The mesh was created using mainly QUAD4 and TRIA3 lower-order elements. The front part of the chassis was created using BECOS beam elements. The rubber mounts in the model were simulated with beam elements. The engine and gear-box of the pick-up were simulated with point mass elements that were positioned on the assumed centre of mass of the components (see figures 7.5 and 7.6). Two iterations were performed on the sub-frame. These iterations were necessary for the following reasons:

- weight reduction,
- compatibility to the swap-body that was still in a development phase, and
- manufacturing aspects.

Various items of the sub-frame had to be modified to make the manufacturing of the sub-frame more cost-effective. These modifications included the holes in the channels, the thickness of the materials and the shape and position of gussets.

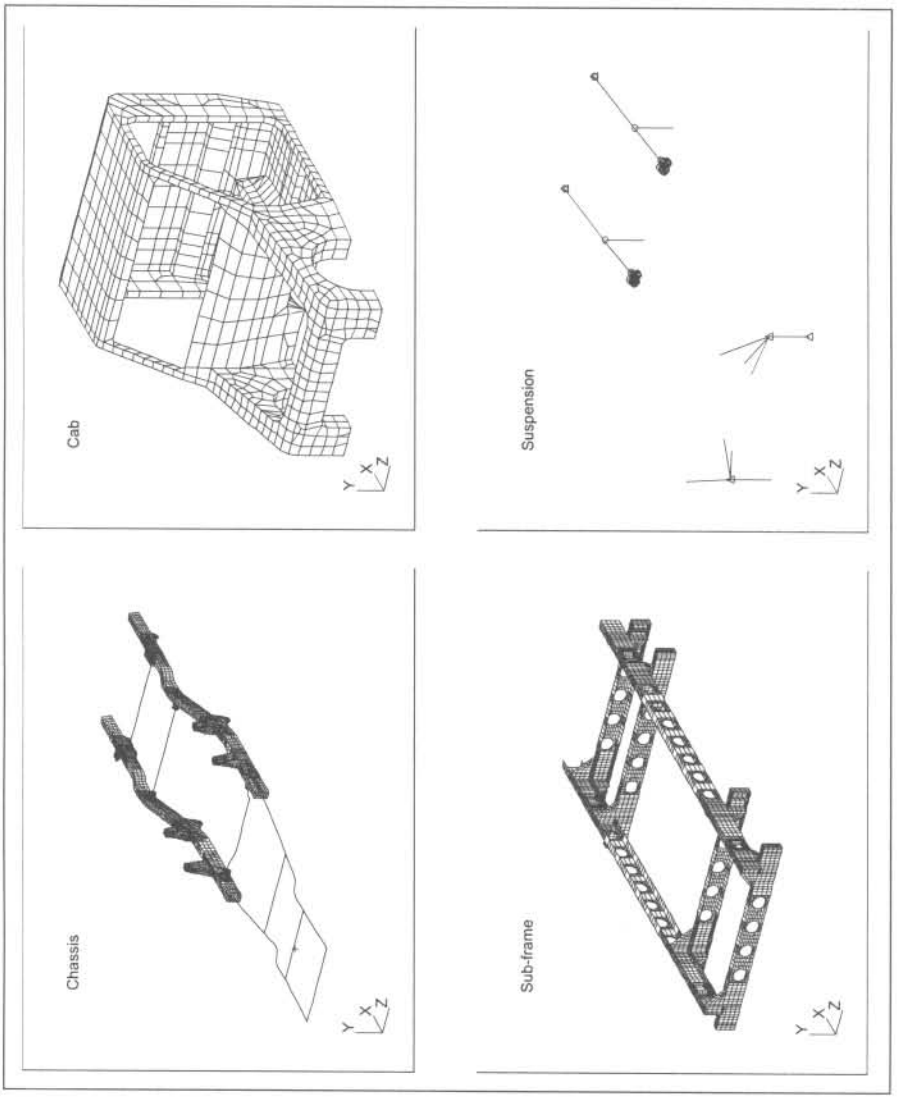

Figure 7.5: Finite Element Model: sub-frame of a pick-up truck

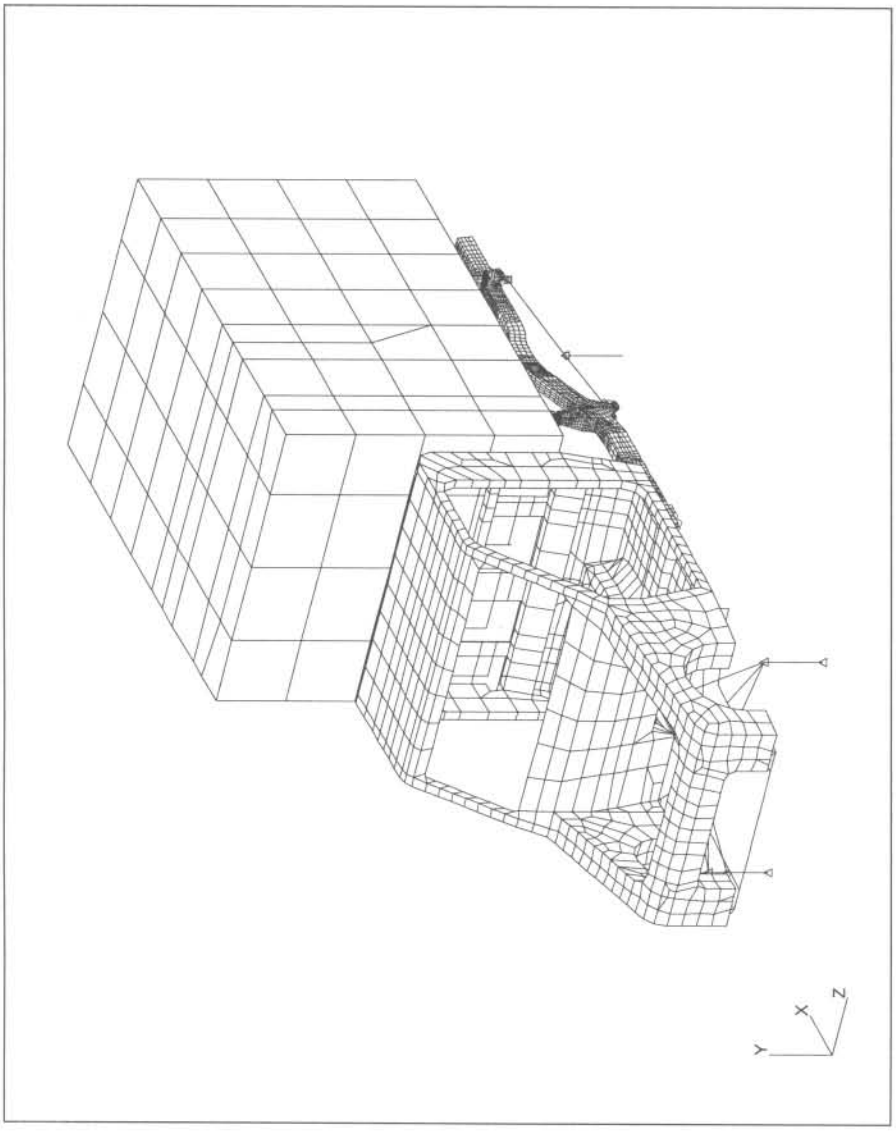

Figure 7.6: Finite Element Model: sub-frame of a pick-up truck

Materials and element properties

The steel chassis, sub-frame and cab elements were defined to have a Young's modulus of 210 GPa and Poisson ratio of 0.3. The prototype swap-body was constructed of aluminum. A Young's modulus of 80 GPa and the Poisson ratio of 0.3 was used. The properties were assigned to the mid-plane of the elements.

Load and Boundary conditions

The pick-up vehicle suspension was simulated with MPC's, beam and rod elements. The suspension was created to simulate the correct bending that the vehicle would have experienced due to vertical and longitudinal loading during the static and dynamic analyses. At the front, MPC's and rods were used to simulate the McPherson-type suspension. The McPherson suspension was connected at the wheel centres to the road surface. At the rear, MPC's were used to model the leaf springs and to connect the wheel centres to the road surface. The model was constrained at the road surface end of the MPC's.

The static analysis made use of a uniformly distributed pressure to simulate a 1 tonne load carried in the swap-body. The initial design iteration analyses had an assumed 2g vertical acceleration applied to the vehicle. The dynamic analyses required a different approach to apply the load. The mass of the swap-body floor elements were increased with a higher density to achieve the correct loading on the sub-frame and chassis. The purpose of the dynamic analysis was to obtain a design criteria for the sub-frame rubbers, so that the swap-body and sub-frame were isolated from the deformations that the chassis experienced. The suspension track data (at a speed of $20km/h$) displayed adequate vertical and torsional displacement on the chassis, and was therefore selected for the dynamic analysis. Due to the small effect of the lateral forces in regard to fatigue damage through the isolation of the sub-frame/swap-body assembly, the lateral loads were omitted from the analysis. The dynamic analysis therefore only used the longitudinal and vertical data to calculate the inputs to the vehicle.

The finite element model was analysed using the PERMAS7 solver for static

analysis and PERMAS4 for the dynamic analysis. The *MSC.Patran* pre- and post-processing software package was used to process the results of the two analysis.

7.4 Suspension bracket of a large passenger bus

Geometry and Finite Element Modelling

The geometry of the suspension bracket was based on the supplied manufacturer's drawing. A bracket specimen was also supplied. The geometry as well as the mesh was created on the *MSC.Patran* FE package. The finite element analysis was done with the PERMAS7 package. The mesh consisted of QUAD4 and TRIA3 lower-order elements. The mesh was created on the centre plane positions of the various plates. Refer to figure 8.5, page 101.

Materials and element properties

The steel bracket was characterised by a Young's modulus of 200 GPa and Poisson ratio of 0.3. The properties were assigned to the mid-plane of the elements. The thickness of the suspension bracket plates were provided by the manufacturing drawings.

Load and boundary conditions

The suspension bracket was suppressed (using MPC's) in all the directions (translational and rotational) at the Huck bolt positions that connect the bracket to the chassis. Two point loads were applied, through MPC's, on the web where the shock absorber is connected to the bracket. A load of $1kN$ was applied on *each* web ($2kN$ in total), in the vertical direction, parallel to the angled plate.

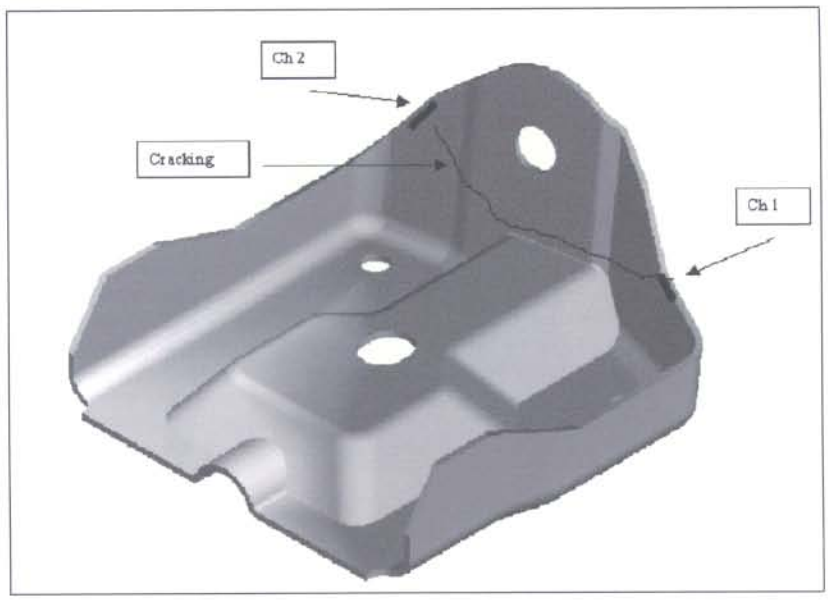

Figure 7.7: Unigraphics solid model - 4x4 pick-up bracket

7.5 Suspension bracket of a 4x4 pick-up truck

Geometry and Finite Element Modelling

The geometry was measured from a physical bracket, and modelled as a solid body in Unigraphics (a CAD package) (refer to figure 7.7). The finite element package *MSC.Patran* was used to create a model of the bracket. Shell elements were used for the model. Refer to the figure 7.8.

Materials and element properties

The steel bracket was characterised by a Young's modulus of 210 GPa and Poisson ratio of 0.3. The properties were assigned to the mid-plane of the elements. The thickness of the component was obtained from the actual component.

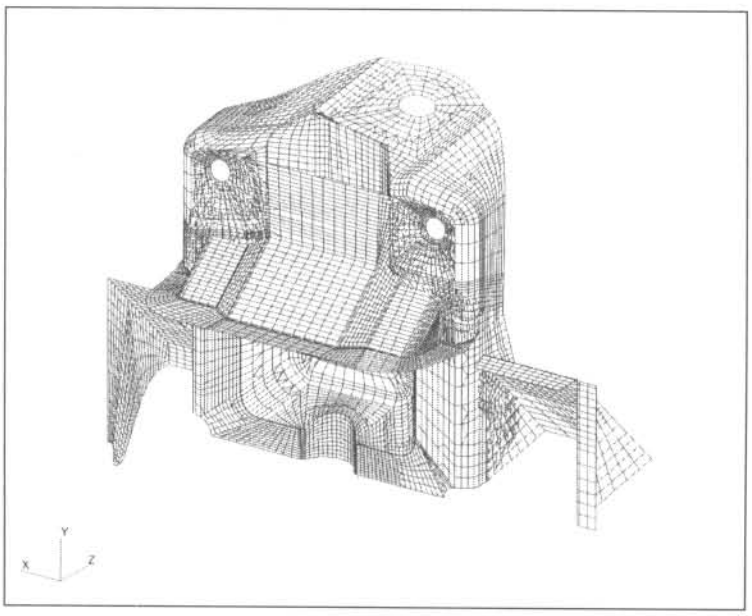

Figure 7.8: Finite element model: bracket of a 4x4 pick-up

Loads and Boundary Conditions

The model was restrained at the edges welded to the chassis beam. A pressure loading perpendicular to the bracket face, was applied to the ring of elements around the mounting hole to simulate the shock absorber force. The total force applied was 212 N. The finite element analysis package, PERMAS was used to analyze the model, performing a linear static analysis. The results of the PERMAS run were evaluated on *MSC.Patran*. Two iterations of design modifications were performed. Firstly, a gusset welded to the mounting face and the back face of the bracket was modelled and assessed. The second iteration involved a U-gusset, welded to the back faces, but only doubling up onto the mounting face, without welding.

7.6 Closure

The finite element models of the various case-studies were discussed in this chapter. The finite element analyses enabled the author to calculate the Fatigue Equivalent Static load. Equally importantly, the finite element tool enables the engineer to use the results of the fatigue analysis for assessment and design purposes.

The following chapter will discuss the results of the assessments of each case-study.

Chapter 8

ASSESSMENT

8.1 Scope

The finite element model enables the engineer, using measurements, to calculate Fatigue Equivalent Static loads for a vehicle structure. The real power of the finite element analysis lies,however, in the ability to assess the structure using the FESL. This chapter deals with the assesments of the finite element analyses.

8.2 Aluminum Dry-bulk Tanker

The results of the analysis performed with PERMAS were evaluated in two parts. High stress areas on the Bulk tanker were identified. These high stress areas were addressed with modifications on the specific part in subsequent analysis (refer to figure 8.1). The first three high stress areas were identified as:

- Certain areas on the tank vessel.
- The kingpin structure, specifically, the rear cross-member.
- At the top of the front boom.

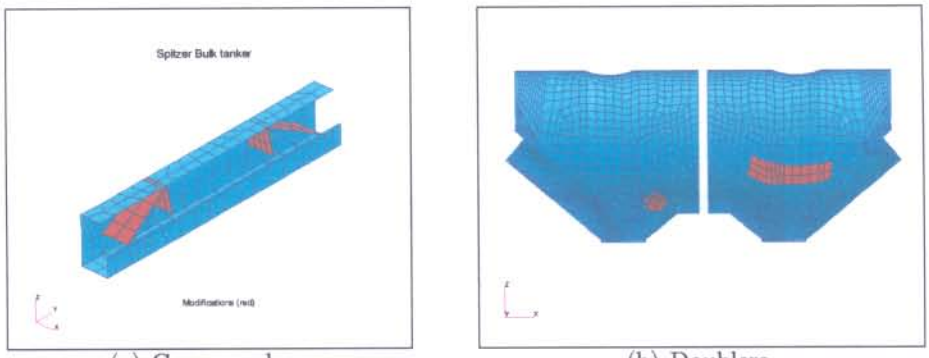

(a) Crossmember (b) Doublers

Figure 8.1: Bulk tanker - Modifications

The high stress areas on the tank vessel were addressed by inserting doublers at strategic positions on the vessel (refer to figure 8.1). Various finite element analyses were done to verify the effectiveness of the additional doublers. An inner bracing was also developed to help alleviate the stresses. The results were plotted for evaluation (refer to figure 8.2).

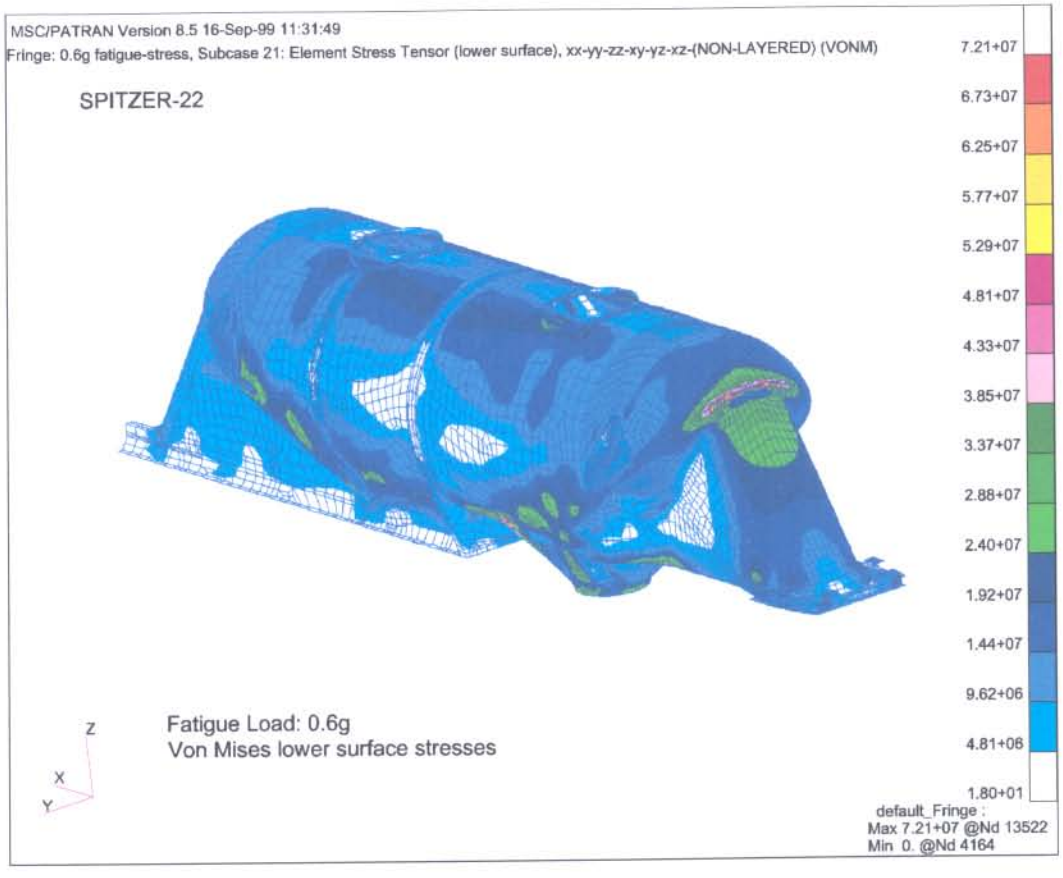

Figure 8.2: Bulk tanker - von Mises stresses

8.3 Sub-frame of a pick-up truck

The static analysis, using the calculated quasi-static fatigue load, indicated that the chassis and the sub-frame would last the design life-time of 200 000km. The finite element analysis of the chassis and sub-frame indicated that no stresses would effect the fatigue strength of the two structures. Stresses of no more than 75 MPa were calculated near the welds on the chassis (refer to figure 8.3). These stresses are well below the weld classifications of the fatigue code [15], and the welded parts would therefore experience no damage during their 200 000km life-time. The sub-frame displayed stresses at some of the welds of approximately 95 MPa. The weld classification of this type of weld is, however, 100 MPa. These welds would therefore last for the designed life-time of 200 000km (refer to figure 8.4).

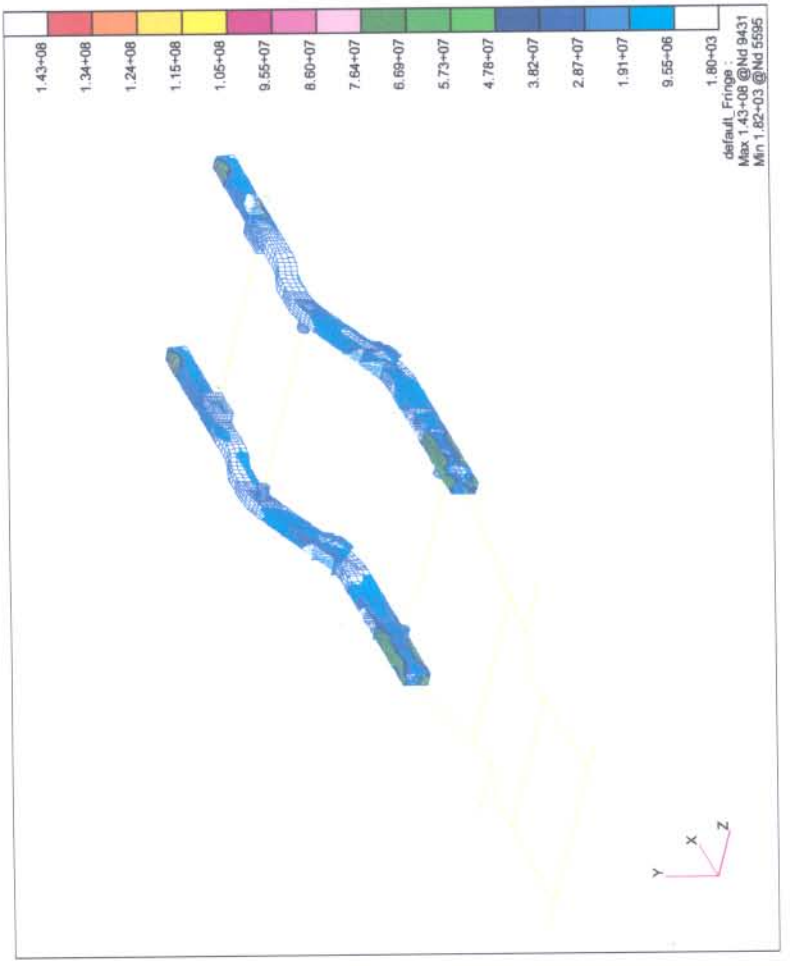

Figure 8.3: Sub-frame: Chassis stresses

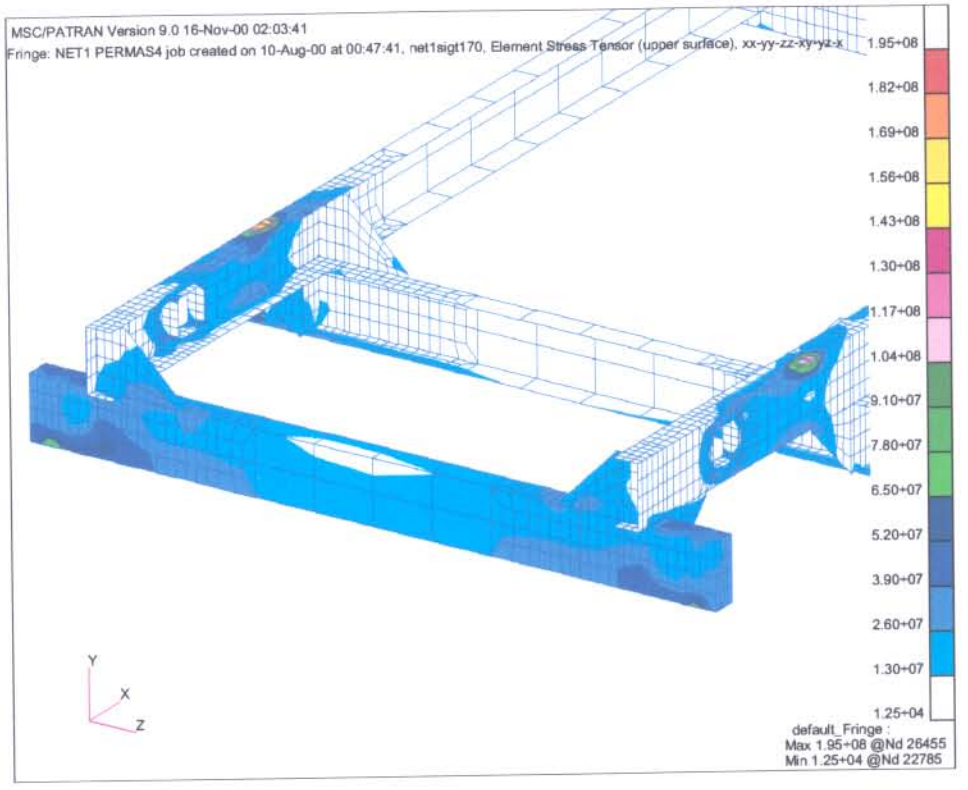

Figure 8.4: Sub-frame: stresses

8.4 Suspension bracket of a large passenger bus

The FE model was subjected to a load of $2kN$. The finite element model consequently showed that the base plate experiences stresses normal to the angled plate in the region of 32 MPa (refer to figure 8.5). A *fatigue equivalent load* of 56.21kN was applied to the model (refer to table 6.7). The new stresses are approximately in the region of 899 MPa. It should be noted that these stresses are fatigue equivalent *stresses*, and the bracket would not actually experience such stresses. According to the ECCS fatigue code [15], the weld that experiences these stresses is a weld with a classification of either 71MPa or 36MPa (an equivalent force of $4.44kN$ and $2.25kN$). A stressed member that falls in the 71 MPa weld classification would endure a nominal stress of 71 MPa for 2×10^6 cycles (refer to section 2.4.3, page 31). The welds on the suspension bracket would fall in the 71 MPa weld category. This is however an optimistic assumption, considering the quality of welds seen on the provided specimen. As mentioned before, the bracket experiences equivalent fatigue stresses of more than 900MPa, while it can only withstand a stress of 71MPa to endure for 2×10^6 cycles (or 3 000 000km). The life time prediction can, however, be calculated for the equivalent fatigue stresses with the stress-life equation 2.6, page 21. According to the fatigue and finite element analysis, using the values from table 6.7 ($56.21kN$, 927MPa), it is predicted that the left suspension bracket would only last approximately 890 cycles or $\pm 1\,350km$ before *crack initiation* would start. The predicted life of the right suspension bracket, using $9.36kN$ and 149.76MPa (refer to table 6.7), would be approximately 213 000 cycles or $\pm$ 320 000 km. These calculations show a close correlation with the actual lifetime of the bracket.

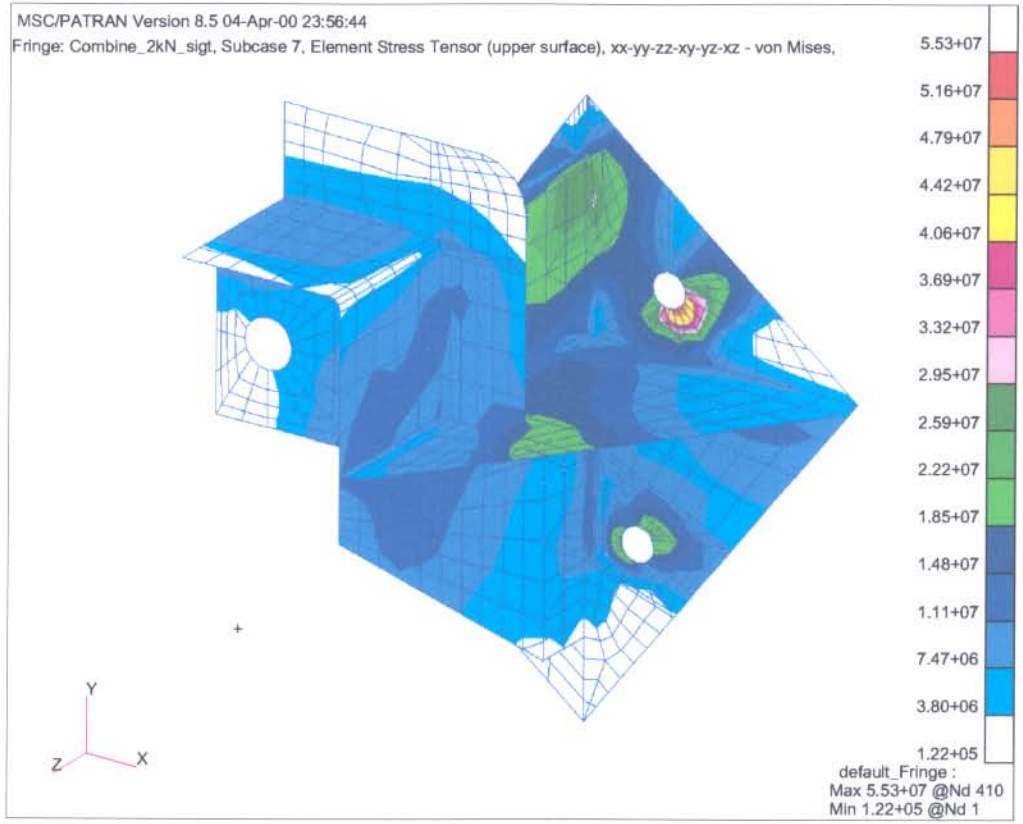

Figure 8.5: Stress results of FEA - bus bracket

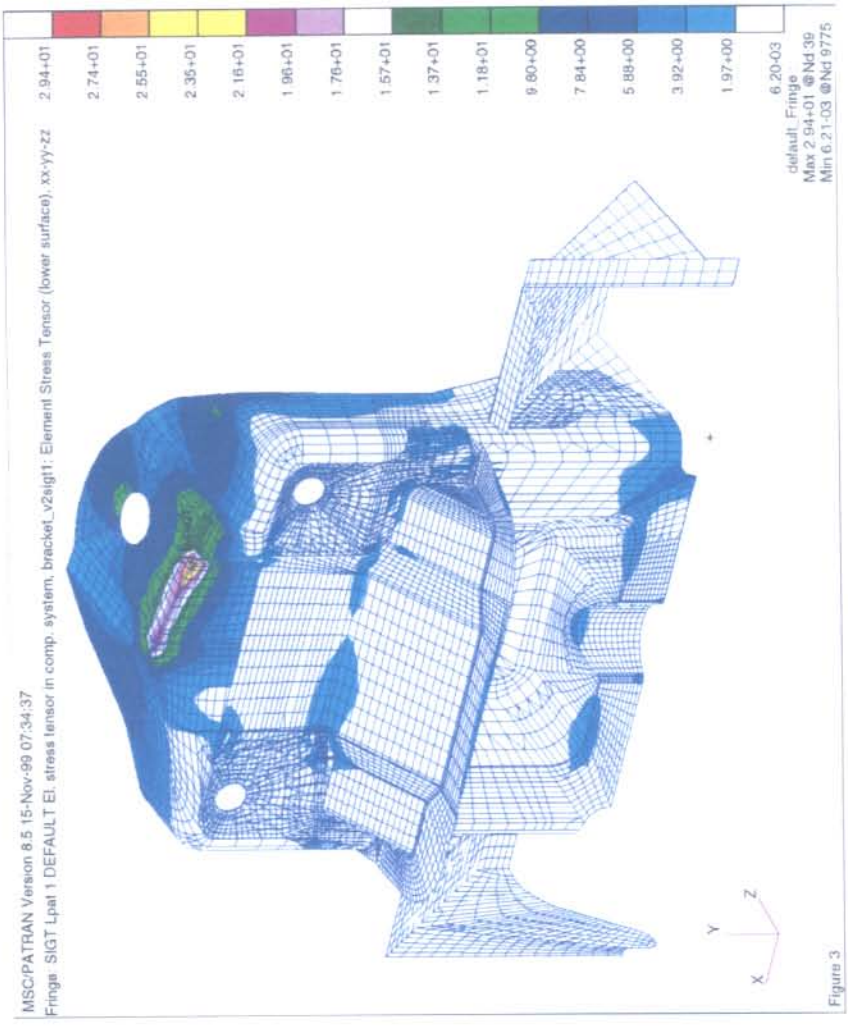

Figure 8.6: Results of FEA: 4x4 pick-up truck bracket

8.5 Suspension bracket of a 4x4 pick-up truck

The front suspension brackets of a 4x4 pick-up truck experienced unacceptable failures during durability testing. Measurements were performed to obtain the loading induced on the shock absorber bracket on the durability test route. A finite element analysis of the original design bracket was performed, resulting in the conclusion that failure is initiated at a stress concentration on a corner between the mounting and back faces of the bracket (refer to figure 8.6). Using the measured data in combination with the finite element results, the fatigue criterion for a modified design was derived. Two iterations of design modifications were performed. Firstly, a gusset welded to the mounting face and the back face of the bracket was modelled and assessed. It became clear from these results that any welding onto the mounting face of the bracket would not achieve the required life expectancy, due to the reduced fatigue strength of a weld. The second design iteration, consisting of an additional U-gusset, welded only to the back face of the bracket, was assessed and found to meet the fatigue criterion. Stresses in the area of the weld were found to be less than 4 MPa and the peak stresses away from the welds on the bracket less than 10 MPa (refer to figure 8.6).

Durability rig testing performed on a baseline (original design) and a prototype modified design specimen, confirmed that the modified design would survive more than 200 000 km of durability route testing. Refer to figures 6.3, 6.4, page 78, 79.

8.6 Closure

In this chapter, the various case-studies were assessed, using the finite element method in conjunction with the static fatigue equivalent load theory. The fatigue load determined for the aluminium bulk tanker, predicted failures on the structure where problems were experienced by the manufacturer. The finite element method enabled the engineers to address the fatigue problems accurately and economically. The sub-frame on the pick-up truck indicated

how powerful the static fatigue equivalent load methodology is during the initial design stages of a vehicle. Various iterations could be performed on the design, without using expensive dynamic analyses and a multitude of testing vehicles. The suspension bracket of the large bus and the 4x4 pick-up truck showed the relative accuracy of the static equivalent fatigue load. During the progress of these case-studies, fatigue life predictions were made and verified against actual field data.

In addition, this chapter also showed how the various structures were analysed and how the structural fatigue problems were solved. The following chapter shall present the conclusion of this study.

Chapter 9

CONCLUSION

The present study aimed to provide an in-depth explanation of the Fatigue Equivalent Static Load methodology. Chapter 3 provided a formulation of the fatigue equivalent static load methodology. Through the use of four case-studies, the method was thoroughly described. Chapter 5 discussed the methods employed to determine the input loads and measurements to the vehicle structures. The fatigue calculations performed on the measurement data were discussed in Chapter 6. Chapter 7 discussed the finite element structural analyses that were performed. The assessment of each of the case-studies was discussed in Chapter 8. The fatigue equivalent static load method has considerable advantages above other methods currently being used in the industry:

1. The fatigue equivalent static load method is flexible enough to be successfully deployed using various methods of input loads. To calculate the static fatigue load, a *relative damage value* is needed at a certain position on the structure. The case-studies in this thesis made exclusive use of time domain strain gauge measurements to ultimately obtain the damage value. However, various other methods can also be used to obtain the damage value (for instance, frequency domain measurements, dynamic analyses and virtual simulations).

2. A Fatigue Equivalent Static Load is structurally *independent*. Theoret-

ically, if two different vehicles are travelling over the same terrain, the resulting FESL analysis would yield exactly the same fatigue load. This is of course only true is the vehicles exhibit similiar dynamic characteristics. Similiar dynamic characteristics would be exhibited by vehicles of approximate the same size and mass (and therefore similiar suspension systems). The Fatigue Equivalent Static Load of two 40 ton trucks would therefore be very similiar, although the structures differ from each other. A design team can therefore use a previously obtained fatigue load to evaluate a new structure without any costly measurement exercises.

3. The fatigue equivalent static load can be incorporated in design codes. This will provide an even more cost-effective method to design and manufacture structures for fatigue loads.

4. The fatigue analysis performed with the use of a FESL is applicable to the complete structure. Positions on a structure that are very difficult to access for measurement purposes can therefore be easily evaluated using a finite element analysis.

The Fatigue Equivalent Static Load method does have a few disadvantages. It is therefore recommended that when this methodology is employed, the following points are considered:

1. The main disadvantage of the FESL method is its inability to address fatigue failures caused by dynamic vibrations. The fatigue load, obtained using the FESL method, subjects a structure to a static deformation. The static deformation would often also correspond to the first global mode shape (eg. chassis under vertical inertial load). The FESL method would therefore take into account dynamic response induced at the first mode. Quasi-static response and excitation frequencies much lower than natural frequencies would also be taken in account. Most of the fatigue related problems that would occur on a structure can be attributed to dynamic response lower that the first mode of bending category. However, loads that excite the structure at higher frequencies would not be

accounted for in the FESL load. An excellent example is shown with the loads calculated on the dry-bulk tanker (see section 6.2, page 66).

The methodology explained by Olofsson et al is especially suited for fatigue analyses caused by dynamic vibrations (see subsection 2.5.5, page 39). Incidently, Olofsson makes use of a very similar methodology to obtain his results (refer to [27]). The Fatigue Damage Response Spectrum (FDRS) method can therefore be successfully combined with the FESL method. The disadvantage of dynamic loads present in higher order bending modes would therefore be solved.

2. Another disadvantage of the FESL method is the use of finite element analysis. Although the finite element analysis procedure is a well established computer aided engineering (CAE) tool, the cost of such an analysis is still more expensive than using, for instance, hand calculations. In addition, a finite element analysis must be done by a person that is experienced and well trained in the use of this tool. The costs of finite element packages are, however, steadily declining. It should be noted that a structure designed with the use of finite element analyses would necessarily yield a much more structurally effective design.

In conclusion, the Fatigue Equivalent Static Load method is an engineering tool that delivers accurate and reliable results to one of the most common structural problems experienced by the industry. The FESL method must however, as with any newly developed engineering tool, be rigorously verified to ensure the robustness of this technique. Complex fatigue loads for vehicle structures do not need to be the main stumbling block of the mechanical design engineer.

Bibliography

[1] Julie A. Bannantine, Jess Comer, and James Handrock. *Fundamentals of Metal fatigue analysis.* Prentice-Hall, Inc., 1990.

[2] K.J. Bathe. *Finite Element Procedures.* Prentice Hall, 1996.

[3] R.S. Beamgard, K.P. Snodgrass, and R.F. Stornant. A field performance prediction technique for light truck structural components. *SAE 791034*, 1979.

[4] T.G. Beckwith, R.D. Marangoni, and J.H. Lienhard V. *Mechanical measurements.* Addison-Wesley Publishing Company, fifth edition edition, 1993.

[5] David Broek. *The practical use of fracture mechanics.* Kluwer Academic Publishers, first edition edition, 1988.

[6] A.A. Butkunas and S.L. Bussa. Quantification of inputs for vehicle system analysis. *SAE 750133*, 1975.

[7] Jr. Charles E. Knight. *The Finite Element Method in Mechanical Design.* PWS-KENT Publishing Company, 1993.

[8] C.-C. Chu. Multiaxial fatigue life prediction method in the ground vehicle industry. *Int. J. Fatigue*, 1997.

[9] Civil Engineering and Building Structures Standards Policy Committee. *Structural use of aluminium*, bs 8118: part 1 edition, 1991.

[10] F.A. Conle and C.-C. Chu. Fatigue analysis and the local stress-strain approach in complex vehicular structures. *Int. J. Fatigue*, vol. 19(1):pp:317–323, 1997.

[11] F.A. Conle and C.W. Mousseau. Using vehicle dynamics simulations and finite element results to generate fatigue life contours for chassis components. *Int. J. Fatigue*, vol. 13:pp:195–205, 1991.

[12] S. Dietz, H. Netter, and D. Sachau. Fatigue life prediction of a railway bogey under dynamic loads through simulation. *Vehicle System Dynamics*, vol. 29:pp. 385–402, 1998.

[13] T. Dirlik. *The establishment of the frequancy domain tranform functions.* PhD thesis, Warwick University, 1985.

[14] K. Dreßler, J. Kötzle, and V.B. Köttgen. Syntheses of realistic loading specifications. *European Journal Mechanical Engineering*, vol. 41(3):pp:153–166, 19xx.

[15] European Convention For Constructional Steelwork. *Recommendations for the Fatigue Design of Steel Structures*, 1st edition, 1985. No. 43.

[16] Ravindran Gopalakrishnan and Hari N. Agrawal. Durability analysis of full automotive body structures. *SAE 930568*, 1993.

[17] V. Grubisic. Determination of load spectra for design and testing. *Int. J. of Vehicle Design*, vol. 15(1/2):pp:8–26, 1994.

[18] T.R. Gurney. Fatigue design rules for welded steel joints. *The Welding Institute Research Bulletin*, vol. 17, 1976.

[19] E. J. Hearn. *Mechanics of Materials.* Butterworth-Heinemann Ltd, second edition edition, 1985.

[20] D.R.H. Jones and K.A. Macdonald. Fatigue failure of a rotating chemical vessel. *Int. J. Fatigue*, pages pp. 77–93, 1996.

[21] Bijan Khatib-Shididi, S. Grewal, and S. Gopalsamy. Durability analysis of pickup truck using non-linear fea. *SAE 962223*, 1996.

[22] Y. Kuo and S.G. Kelkar. Body-structure durability analysis. *Automotive Engineering*, 1995.

[23] C. Leser, S. Thangjitham, and N.E. Dowling. Modeling of random vehicle loading histories for fatigue analysis. *Int. J. of Vehicle Design*, vol. 15, 1993.

[24] The MacNeal-Schwendler Corporation. *MSC/FATIGUE Version 6*, no. 903030 edition, 1996.

[25] M. Matsuishi and T. Endo. Fatigue of metals subjected to varying stress. *Proc. Kyushu Branch of Japan. Soc. of Mech. Eng.*, pages pp:37–40, 1968.

[26] Michel Olagnon. Practical computation of statistical properties of rainflow counts. *Int. J. of Fatigue*, vol. 16:pp. 306–314, 1994.

[27] U. Olofsson, T. Svensson, and H. Torstensson. Response spectrum methods in tank-vehicle design. *Experimental Mechanics*, 1995.

[28] R.E. Poutney and J.D. Dakin. Integration of test and analysis for component durability. *Environmental Engineering*, vol. 5(2):pp:13–17, 1992.

[29] A. Rahman. Toward reliable finite element analysis. *Environmental engineering*, 1997.

[30] H.S. Reemsnyder. Hot-spot stress approach to fatigue design of weldments. *SAE-University of Iowa, Short course notes of fatigue concepts in Design*, 1986.

[31] Y Rui, R.S. Borsos, and et. al. The fatigue life prediction method for multi-spot-welded structures. *SAE 930571*, 1993.

[32] Frank Sherrat. Current applications of frequency domain fatigue life estimation. In *Product Optimization for Integrity*, 1995.

[33] Joseph E. Shigley. *Mechanical Engineering Design.* McGraw-Hill Book Company, first metric edition edition, 1986.

[34] M. Slavik and J. Wannenburg. Prognosis of vehicle failure due to fatigue. In R.K. Penny, editor, *Risk, Economy and Safety, Failure minimisation and Analysis*, 1998.

[35] R.A. Smith and J.F. Cooper. Theoretical predictions of the fatigue life of shear spot welds. In S. J. Maddox, editor, *Fatigue of Welded Structures.* The Welding Institute, 1988.

[36] South African Bureau of Standards. *Road tank vehicles for petroleum based flammable liquids*, 1994. 1398.

[37] R.I. Stephans, B. Dopker, E.J. Baek, L.P. Johnson, and T.S. Liu. Computational fatigue life prediction of welded and non-welded ground vehicle components. *SAE 871967*, 1987.

[38] United Kingdom Department of Energy. *Offshore installations: Guide on Design and Construction*, 1st edition, 1984.

[39] J. Wannenburg. *The establishment of input loading for automotive and transport structures.* PhD thesis, University of Pretoria, 2003.

[40] Welding Standards Policy Committee. *British Standard: Fatigue design and assesment of steel structures*, 1st edition, 1993. BS 7608: 1993.